Journal for ImmunoTherapy of Cancer

B cells imprint adoptively transferred CD8$^+$ T cells with enhanced tumor immunity

Aubrey S Smith ,[1,2,3] Hannah M Knochelmann,[1,2,3] Megan M Wyatt,[2,3] Guillermo O Rangel Rivera,[1,2,3] Amalia M Rivera-Reyes,[2,3] Connor J Dwyer,[1] Michael B Ware,[2,3] Anna C Cole,[2,3] David M Neskey,[4,5] Mark P Rubinstein,[6] Bei Liu,[7] Jessica E Thaxton,[8,9] Eric Bartee ,[10] Chrystal M Paulos[1,2,3]

To cite: Smith AS, Knochelmann HM, Wyatt MM, *et al*. B cells imprint adoptively transferred CD8$^+$ T cells with enhanced tumor immunity. *Journal for ImmunoTherapy of Cancer* 2022;**10**:e003078. doi:10.1136/jitc-2021-003078

► Additional supplemental material is published online only. To view, please visit the journal online (http://dx.doi.org/10.1136/jitc-2021-003078).

Accepted 29 November 2021

For numbered affiliations see end of article.

Correspondence to
Aubrey S Smith;
aubrey.s.smith@emory.edu

Dr Chrystal M Paulos;
chrystal.mary.paulos@emory.edu

ABSTRACT

Background Adoptive T cell transfer (ACT) therapy improves outcomes in patients with advanced malignancies, yet many individuals relapse due to the infusion of T cells with poor function or persistence. Toll-like receptor (TLR) agonists can invigorate antitumor T cell responses when administered directly to patients, but these responses often coincide with toxicities. We posited that TLR agonists could be repurposed ex vivo to condition T cells with remarkable potency in vivo, circumventing TLR-related toxicity.

Methods In this study we investigated how tumor-specific murine CD8$^+$ T cells and human tumor infiltrating lymphocytes (TILs) are impacted when expanded ex vivo with the TLR9 agonist CpG.

Results Herein we reveal a new way to reverse the tolerant state of adoptively transferred CD8$^+$ T cells against tumors using TLR-activated B cells. We repurposed the TLR9 agonist, CpG, commonly used in the clinic, to bolster T cell—B cell interactions during expansion for ACT. T cells expanded ex vivo from a CpG-treated culture demonstrated potent antitumor efficacy and prolonged persistence in vivo. This antitumor efficacy was accomplished without in vivo administration of TLR agonists or other adjuvants of high-dose interleukin (IL)-2 or vaccination, which are classically required for effective ACT therapy. CpG-conditioned CD8$^+$ T cells acquired a unique proteomic signature hallmarked by an IL-2Rα^{high}ICOS^{high}CD39^{low} phenotype and an altered metabolic profile, all reliant on B cells transiently present in the culture. Likewise, human TILs benefitted from expansion with CpG ex vivo, as they also possessed the IL-2Rα^{high}ICOS^{high}CD39^{low} phenotype. CpG fostered the expansion of potent CD8$^+$ T cells with the signature phenotype and antitumor ability via empowering a direct B–T cell interaction. Isolated B cells also imparted T cells with the CpG-associated phenotype and improved tumor immunity without the aid of additional antigen-presenting cells or other immune cells in the culture.

Conclusions Our results demonstrate a novel way to use TLR agonists to improve immunotherapy and reveal a vital role for B cells in the generation of potent CD8$^+$ T cell-based therapies. Our findings have immediate implications in the clinical treatment of advanced solid tumors.

BACKGROUND

Only a decade ago, the treatment options for patients diagnosed with late-stage solid malignancies were mostly ineffective and patient outcomes were bleak. With the advent of immunotherapies, including checkpoint blockade and adoptive T cell transfer (ACT) therapy, a new era of cancer care is underway. Many patients with advanced cancer, like metastatic melanoma, experience objective responses, undergo long-term remissions and can sometimes be cured of their disease following delivery of T cell-based therapies.[1] However, as some patients receive ACT as a last resort, after progressing on multiple lines of therapy, and only 20% experience durable complete responses, it is paramount to find ways to improve cell therapy.[1] Host preconditioning with chemotherapy or radiotherapy is critical to the success of ACT. The preconditioning regimen promotes engraftment and antitumor activity of transferred T cells.[2] Beyond depletion of host immune cells that compete for homeostatic cytokines and/or suppress transferred cells (T regulatory cells or myeloid-derived suppressor cells), host preconditioning also alters gut microbiota homeostasis.[3–5] The systemic release of gut microbes and microbial products, via Toll-like receptor (TLR) ligands, in turn, activates the innate immune system and augments the effectiveness of infused T cells via pathogen recognition receptors.[6]

Additional insights from the microbiome field have led to improvements in immunotherapy, such as the use of TLR ligands to induce immunity.[7 8] We and other groups have shown that TLR activation via synthetic microbial ligands improves ACT therapy when administered directly to mice.[9 10] While these findings are important, delivering TLR agonists alongside ACT therapy may induce

toxic side effects in patients and delivering TLR ligands in vivo may induce unwanted effects on other immune cells or even tumor cells.[11] Although TLR agonists can profoundly augment immunotherapy, the safest and most effective ways to use them for ACT remain unknown.

CpG DNA agonists of TLR9 have been widely used in both preclinical and clinical settings in combination with various therapies (eg, vaccines, checkpoint blockade therapies, immune-agonistic antibodies, chemo/radiation) and as a monotherapy to induce antitumor responses (NCT03445533, NCT03618641, NCT03007732, NCT03831295, NCT03410901).[12–20] Initially, several clinical trials reported activation of immune cells in patients with TLR9 agonist administration, but few individuals experienced a complete durable antitumor response.[21] Three recent trials, however, reported patient responses (partial response and complete response) to TLR9 agonists in combination with either low-dose local irradiation of a single tumor site, pembrolizumab, or ipilimumab.[15 18 22] Importantly, all three reports noted treatment-emergent adverse events (AEs) of grade 3 and/or 4 in a portion of the patients. In these and other reports, CpG is directly administered to the patient and the route and timing of treatment are likely important.[23] CpG is typically administered locally to tumor lesions, either subcutaneously or intratumorally, in clinical trials to promote targeted action to the tumor and avoid bioavailability issues that arise with systemic intravenous injection.[23] While local administration strategies such as these may be a valuable therapeutic option for some patients, they do somewhat limit the patient population to those with readily accessible tumor sites. Further, as severe AEs arise in many patients treated with combination therapies which include TLR9 agonist administration, determining the best way to exploit these agonists therapeutically while bypassing in vivo toxicity is paramount.

Herein, we developed a novel method in which CpG promotes efficacy of cell therapy without in vivo administration. We hypothesized that the efficacy of T cells could be improved by incorporating a TLR9 agonist into the ex vivo expansion protocol. This approach obviates the need to determine route and timing of CpG delivery and negates any unwanted off-target effects of CpG in vivo. ACT with $CD8^+$ T cells expanded with CpG was effective without in vivo interleukin (IL)-2 and vaccine adjuvants, which are typically necessary. To our surprise B cells played an essential role in imprinting $CD8^+$ T cells with potent immunity. Overall, we describe how addition of CpG in culture propagates $CD8^+$ T cells which display overt immunity against solid tumors in vivo and reveal mechanisms underlying their potency.

METHODS

Mice and tumor cell lines

Pmel-1 TCR transgenic mice were purchased from the Jackson Laboratories and bred in the in-house animal facilities (comparative medicine department) at the Hollings Cancer Center of the Medical University of South Carolina (MUSC) or Emory University. C57BL/6 mice were purchased from Jackson laboratories for use in in vivo tumor experiment studies. Mice used for tumor experiments were between 6 and 10 weeks old. All animals were housed and underwent experimentation in accordance with the Institutional Animal Care and Use Committee (IACUC) at MUSC or Emory, and under the supervision and support of the Division of Laboratory Animal Resources at MUSC or the Division of Animal Resources at Emory. IACUC approval was obtained prior to all animal studies and procedures. B16F10 ($H\text{-}2^b$) melanoma and $B16F10^{KVP}$ cell lines were gifted from Nicholas P. Restifo for use in in vivo tumor studies.[24] Cell lines were confirmed pathogen and mycoplasma free prior to use in experimental studies.

T cell culture

Pmel-1 cells

Pmel-1 transgenic T cells were obtained via the culture of whole pmel-1 splenocytes. Pmel-1 splenocytes were seeded at $1e^6$/mL in a 24-well plate and activated with 1 µM human gp100 (hgp100) peptide (unless indicated otherwise) in the presence of 100 IU/mL IL-2 (NIH repository). At the time of activation (unless otherwise stated) either mouse CpG-ODN 1668 (5'-tccatgacgttcctgatgct-3') (class B) was added to the culture at 0.5 µg/mL or vehicle control (endotoxin-free water) was added at a matched volume (InvivoGen). On day 2 of culture, half of the culture media was replaced with fresh media with 100 IU/mL IL-2 in the new media. From day 3 of culture on cells were split to a concentration of $1e^6$ cells/mL and supplemented with fresh media containing 100 IU/mL IL-2. On day 7 of culture, T cell cultures were assayed using flow cytometry and then directly used for in vivo tumor experiments where indicated.

$CD8^+$ T cell negative isolation

For experiments in which T cells were purified from the bulk pmel-1 splenocytes before culturing we used the EasySep Mouse $CD8^+$ T cell Isolation Kit (Stem Cell, Cat# 19853A) following the manufacturer's protocol. Prior to cell culture, the T cell isolate was assayed for the purity of the product which was always more than 90% pmel-1 transgenic T cells (identified via expression of the Vβ13 chain of the TCR).

In vitro blockade of soluble factors or CD40L

Pmel-1 splenocyte cultures were established. Prior to activating with hgp100 peptide, IL-2 (100 IU/mL) and adding CpG or vehicle control, antibodies directed against IFN-γ (BioXCell BE0312), IL-6 (BioXCell BE0046), Timp-1 (R&D AF980), CXCL10 (R&D AF-466-NA), IL-10 (BioXCell BE0049) or relevant isotype controls (IgG1 (BioXcell BE0088), polyclonal Armenian hamster IgG (BioXCell BE0091), Normal Goat IgG (R&D AB-108-C)) were added to cell culture at 10 µg/mL. Blocking antibody for CD40L (BioXCell BE0017-1) or isotype control Armenian

hamster IgG (BioXCell BE0091) antibody was added to cell culture at 25 µg/mL. Antibodies were added every day for the duration of cell culture and IL-2 was added at 100 IU/mL in fresh media whenever cells were split.

Supernatant transfer

Cell culture supernatant was collected from bulk pmel-1 splenocytes activated with hgp100 peptide, IL-2 and treated with vehicle or CpG at 7, and 48 hours post seeding, spun down to remove any cells, and stored at −20°C. Fresh pmel-1 splenocytes or isolated $CD8^+$ T cells (Stem Cell, Cat# 19853A) were resuspended in supernatants, after supernatants were thawed and at room temperature. Additional IL-2 (100 IU/mL) and hgp100 were added to activate cell cultures and pmel-1 T cells were expanded for 7 days. Control cell cultures were established concomitantly by activating with hgp100 peptide, IL-2, and fresh CpG or vehicle control.

Bypass antigen-presenting cells

To bypass antigen-presenting cell (APC) mediated activation of pmel-1 T cells (via major histocompatibility complex (MHC) class I presentation of peptide to the TCR) we used bead-bound or plate-bound antibodies. αCD3/αCD28 beads from Gibco (DynaBeads 11453D) were added at the start of culture at 1:1 ratio of beads to pmel-1 cells. Cell culture plates were coated overnight with αCD3 alone or αCD3 and αCD28 (10 µg/mL αCD3 and 2 µg/mL αCD28) in sterile phosphate-buffered saline (PBS) at 4°C and used the next day for cell culture after gently washing the wells with sterile PBS. Control pmel-1 cultures were activated with hgp100 peptide and all groups received 100 IU/mL IL-2 and CpG or vehicle control as in previous assays.

Immune cell subset depletion

From the bulk pmel-1 splenocytes we depleted either $CD4^+$ T cells, natural killer (NK) cells, dendritic cells (DCs), macrophages, or B cells using subset marker-specific PE labeling followed by anti-PE microbead targeting and positive selection via column isolation. The negative fraction was used for culture as it does not contain the positively labeled cell subset. Briefly, pmel-1 splenocytes are labeled with PE-conjugated antibodies: either αCD4-PE, αNK1.1-PE, αCD11c-PE, αF4/80-PE, or αCD19-PE (antibodies listed in table 1) to mark $CD4^+$ T cells, NK cells, DCs, macrophages, or B cells, respectively. Cell mixtures were then further labeled with Anti-PE MicroBeads from MACS Miltenyi Biotec (130-048-801) and then underwent magnetic separation with the MACS LS Columns (130-042-401) according to the manufacturer's instructions. Both positive and negative fractions were collected into 15 mL tubes, and assayed via flow cytometry for the presence of the PE-conjugated cell specific marker as well as another secondary marker, when applicable, to identify the presence of each subset in each fraction. The average per cent depletion of each subset or dual depletion was as follows: 97.6, 94.4, 99.8, 98.8, 82.2, and 96.9 of $F4/80^+$ macrophages, $CD11c^+$ DCs, $CD19^+$ B cells, $CD4^+$ T cells, $NK1.1^+$ NK cells and $F4/80^+$ macrophages/$CD11c^+$ DCs dual depletion, respectively. The negative fraction was cultured as described above, using hgp100 peptide activation, 100 IU/mL IL-2, vehicle or CpG treatment on day 0. Bulk pmel-1 splenocytes were cultured in the same manner as controls.

B cell negative isolation

B cells were negatively isolated using the EasySep Mouse B cell Isolation Kit (Stem Cell, Cat# 19854) following the manufacturer's instructions. B cell purity was assayed post isolation and prior to cell culture with purified $CD8^+$ T cells. In recombination experiments, $CD8^+$ T cells were cultured with B cells at a 1:4 T:B cell ratio and activated and expanded in culture as described above.

Human oral cavity squamous cell carcinoma (OCSCC) tumor infiltrating lymphocyte culture

Our tumor infiltrating lymphocyte (TIL) culture method was adapted from the method reported by Dudley *et al*.[25] Briefly, tumor specimen was collected fresh from a patient with oral cavity squamous cell carcinoma and cut into 1–3 mm^2 fragments before seeding in complete media (RPMI) supplemented with 6000 IU/mL recombinant IL-2 (NCI repository). At the time of seeding three tumor fragments were additionally treated with either vehicle control (endotoxin-free water) or CpG ODN 2006 (InvivoGen) at 0.5 µg/mL. Tumor fragments were left untouched for 5 days in culture to allow cell egress from the tumor piece. After 5 days 1 mL/well (24-well plate) was removed without disturbing the cells settled on the bottom of the well and replaced with fresh media with 6000 IU/mL IL-2. Cells were monitored and media was replaced every 3–5 days. Once cells became confluent in the well, the tumor piece was removed and cells were replated and maintained at 1–1.5×10^6 cells/mL in a 24-well plate.

Adoptive cell therapy

Tumor cells (B16F10 or $B16F10^{KVP}$) cells from culture were washed twice, resuspended in sterile PBS, and injected subcutaneously on the abdomen at $5e^5$ cells/mouse (in 200 µL). Tumors were established for 5 days (unless otherwise noted in the figure legend) in vivo prior to ACT and mice were irradiated with 4–5 Gy total body irradiation the day before ACT. Prior to treatment, mice were randomized according to tumor size to distribute tumor size evenly among groups. Average tumor size for parental B16F10 tumors was 25 mm^2 among mice on the day of cell therapy (D0) unless otherwise indicated in the figure legend. If no tumor was detectable 4 days post tumor cell injection, mice were not included in the study. $5e^6$ pmel-1 cells expanded 1 week in vitro were resuspended in sterile PBS and transferred via tail vein injection (unless cell number noted otherwise in the figure legend). Starting from day 0 of ACT, tumors were measured 2× per week with handheld calipers by a laboratory member blinded to the treatment

Table 1 List of antibodies

Target (anti-mouse)	Clone	Fluorophore	Manufacturer	Catalog number
CD8	53–6.7	PerCpCy5.5	Biolegend	100734
	53–6.7	PE	BD Biosciences	553033
CD4	GK1.5	APC Cy7	BD Biosciences	552051
Vβ13	MR12–3	APC	BD Biosciences	561542
Thy1.1	OX-7	APC Cy7	Biolegend	202520
B220	RA3-62B	APC	Invitrogen	17-0452-82
MHC II	M5/114.15.2	PE	Biolegend	107607
CD11c	N418	BV41	Biolegend	117343
	HL3	PE	BD Biosciences	557401
F4/80	BM8	PeCy7	Biolegend	123113
	T45-2342	PE	BD Biosciences	565410
NK1.1	PK136	FITC	BD Biosciences	553164
	PK136	PE	BD Biosciences	557391
CD19	1D3	PE	BD Biosciences	553786
IL-2Rα	7D4	FITC	BD Biosciences	553072
	PC61	PE	BD Biosciences	553866
ICOS	C398.4A	BV421	Biolegend	313524
CD39	Duha59	Pe-Cy7	Biolegend	143806
CD44	IM7	PerCp-Cy5.5	Biolegend	103032
TLR9	M9.D6	FITC	Invitrogen	11-9093-80
CD3	17A2	eflour450	eBioscience	48-0032-82
CD64	X54-517.1	Pe-Cy7	Biolegend	139313
IFN-γ	H22	NA	BioXCell	BE0312
IL-6	MP5-20F3	NA	BioXCell	BE0046
Timp-1	Polyclonal Goat IgG	NA	R&D	AF980
CXCL10	Polyclonal Goat IgG	NA	R&D	AF-466-NA
IL-10	JES5-2A5	NA	BioXCell	BE0049
CD40L	MR-1	NA	BioXCell	BE0017-1
Isotype: IgG1	HRPN	NA	BioXCell	BE0088
Isotype: Polyclonal Armenian hamster IgG	NA	NA	BioXCell	BE0091
Isotype: Polyclonal goat IgG	NA	NA	R&D	AB-108-C
Target (anti-human)	**Clone**	**Fluorophore**	**Manufacturer**	**Catalog number**
CD8	RPA-T8	PerCp-Cy5.5	Biolegend	301032
CD4	RPA-T4	PE	eBioscience	12-0049-42
ICOS	4B4-1	V450	Biolegend	309819
IL-2Rα	BC96	APC-Cy7	Biolegend	302614
CD39	A1	PE-Cy7	Biolegend	328212

APC, antigen-presenting cell; IFN, interferon ; IL, interleukin; TLR, Toll-like receptor .

group until tumors reached protocol endpoint (400mm^2). Mice euthanized prior to endpoint for tissue collection and biodistribution analysis were identified and allocated prior to commencing treatment.

Mouse blood and tissue collection

Peripheral blood

Mouse peripheral blood was collected at the indicated time points post ACT from the mandibular vein into 1.5 mL Eppendorf tubes containing 0.125 M EDTA. All blood was pelleted, and red blood cells were lysed using RBC Lysis buffer (Biolegend). Immune cells were then assayed via flow cytometry.

Tumor collection

Tumors were excised and placed in culture media on ice until tissue dissociation. Tumor single cell suspensions were acquired using the MACS mouse Tumor

Dissociation Kit (130-096-730), following the manufacturer's instructions, and the gentle MACS Octo Dissociator with Heaters. The single cell suspension was washed with FACs buffer (PBS+2% HI-FBS) and filtered over a 70 µM screen and collected into 50 mL tubes. Cell suspensions were further filtered through a 40 µM filter prior to flow cytometry analysis to prevent clumping. $V\beta13^{+}CD8^{+}$ or $Thy1.1^{+}$ staining was used to detect pmel-1 donor $CD8^{+}$ T cells in the peripheral blood and tissues.

Proteomics

Sample preparation

Four biological replicates of day 7 T cells from vehicle or CpG-treated cultures were collected, washed with sterile PBS, and pelleted. Cells were lysed in 9M urea, 50 mM Tris pH 8, with 100 units/mL Pierce Universal Nuclease (Thermo Scientific) added. The concentration of protein was measured using the BCA assay (Thermo Scientific). Fifty micrograms of protein from each sample were brought to the same final volume using the lysis buffer and reduced in 1 mM 1,4-dithiothreitol, and alkylated in 5.5 mM iodoacetamide (both from Thermo Scientific). The urea concentration was then reduced to 1.6M using 50 mM ammonium bicarbonate. The samples were digested with Lys-C (Waco) at a 1:50 protease: protein ratio for 3 hours at room temperature followed by trypsin (Sigma) at 37°C for 18 hours at a 1:50 protease: protein ratio. The resulting peptides were desalted using C18 Stage Tips (Thermo Scientific) using a standard protocol. The elution from the stage tip for each sample was dried in a Speed Vac and stored at −80°C.

Liquid chromatography and mass spectrometry data acquisition parameters

Dried peptides were dissolved in 15 µL of 2% acetonitrile (ACN)/0.2% formic acid (FA) and 5 µL of this was injected. Peptides were separated and analyzed on an EASY nLC 1200 System (Thermo Scientific) in line with the Orbitrap Fusion Lumos Tribrid mass spectrometer (Thermo Scientific) with instrument control software V.4.2.28.14. Peptides were pressure loaded at 1180 bar, and separated on a C18 reversed phase column (Acclaim PepMap RSLC, 75 µm×50 cm (C18, 2 µm, 100 Å)) (Thermo Fisher) using a gradient of 2%–35% B in 180 min (Solvent A: 0.1% FA, 2% ACN; Solvent B: 80% ACN/0.1% FA) at a flow rate of 300 nL/min. The column was thermostated at 45°C. Mass spectra were acquired in data-dependent mode with a high resolution (60,000) Fourier transform mass analyzer (FTMS) survey scan, mass range of m/z 375–1575, followed by tandem mass spectra (MS/MS) of the most intense precursors with a cycle time of 3 s. The automatic gain control target value was 4.0e5 for the survey scan. Fragmentation was performed with a precursor isolation window of 1.6 m/z, a maximum injection time of 50 ms, and higher-energy collisional dissociation (HCD) collision energy of 35%; the fragments were detected in the Orbitrap at a 15,000 resolution. Monoisotopic-precursor selection was set to 'peptide'. Apex detection was not enabled. Precursors were dynamically excluded from resequencing for 15 s with a mass tolerance of 10 ppm. Advanced peak determination was not enabled. Precursor ions with charge states that were undetermined, 1, or >7 were excluded from fragmentation.

Mass spectrometry data processing

Protein identification and quantification were extracted from raw LC-MS/MS data using the MaxQuant platform V.1.6.3.3 with the Andromeda database searching algorithm and label-free quantification (LFQ) algorithm.[26–28] Data were searched against a mice Uniprot reference database UP000000589 with 54425 proteins (April, 2019) and a database of common contaminants. The false discovery rate (FDR), determined using a reversed database strategy, was set at 1% at the protein and peptide level. Fully tryptic peptides with a minimum of seven residues were required including cleavage between lysine and proline. Two missed cleavages were permitted. The LFQ feature was on with 'Match between runs' enabled for those features that had spectra in at least one of the runs. The 'stabilize large ratios' feature was enabled, and 'fast LFQ' was disabled. The first search was performed with a 20ppm mass tolerance; after recalibration, a 4.5 ppm tolerance was used for the main search. A minimum ratio count of 2 was required for LFQ protein quantification with at least one unique peptide. Parameters included static modification of cysteine with carbamidomethyl and variable N-terminal acetylation and oxidation of methionine. The protein groups text file from the MaxQuant search results was processed in Perseus V.1.6.8.0.[29] Identified proteins were filtered to remove proteins only identified by a modified peptide, matches to the reversed database, and potential contaminants. The normalized LFQ intensities for each biological replicate were log2 transformed. Quantitative measurements were required in at least two out of three biological replicates in at least one of the treatment groups. Gene ontology and Reactome pathway annotations were added from the murine Uniprot reference proteome. The mass spectrometry proteomics data have been deposited to the ProteomeXchange Consortium via the PRIDE[30] partner repository with the data set identifier PXD022909. Principal component analysis (PCA) analysis was performed in Perseus. A volcano plot was generated in Perseus using a significance threshold of a two-sided t-test adjusted p value (<0.05 FDR) and a S0 parameter of 0.1. Protein set enrichment analysis was performed using the ToppFun function of the ToppGene Suite (https://toppgene.cchmc.org/enrichment.jsp), where the proteins increased significantly (two-sided t-test adjusted p value (<0.05 FDR) and a S0 parameter of 0.1) were assessed.

Flow cytometry

Flow cytometry was performed on either a BD FACSVerse, BD LSRFortessa X-20, or BD FACSymphony A3 instrument and subsequently analyzed using FlowJo software (BD).

For extracellular staining, cells were suspended in FACS Buffer (PBS+2% FBS) and incubated with antibodies against cell surface markers (indicated in table 1) and Zombie Aqua viability dye for 20 min at room temperature or 30 min at 4°C. TMRM (250 nM) and MitoTracker Deep Red (20 nM) staining were done at 37°C and room temperature, respectively. For intracellular staining, after cell surface staining cells were fixed (BD) for 15 min at room temperature, permeabilized (BD) for 20 min at room temperature, and incubated for an additional 20 min with antibodies against target proteins in perm buffer at room temperature. Cells were then washed with FACS Buffer prior to running on either flow cytometer.

Immunological Genome Project database query

Murine *Tlr9* transcript expression was assessed in multiple immune cell types using the online database of the Immunological Genome Project (ImmGen) (https://www.immgen.org/). We queried the ImmGen ULI RNA sequencing database under the Gene Skyline databrowser.

Statistics

Graphs and statistical analyses were created and performed in GraphPad Prism V.7 or Perseus for proteomics analyses. Survival was compared using a Log-rank (Mantel-Cox) test. To compare two treatment groups, we used either a two-sample t-test or a Mann-Whitney U test as indicated in figure legends. A priori statistical projections were used to calculate the number of host mice needed for engraftment and persistence experiments. For these longitudinal assays the minimum number of mice/treatment group was calculated to be six mice which allowed us to achieve 80%–95% power (two-sided α of 0.05). In average tumor curves each point signifies the average tumor area at that time and the error bars indicate SEM. In dotplots of replicate analyses mean and SD are indicated. P values less than 0.05 were considered significant. To identify significantly regulated proteins a Student t-test was performed with a permutation-based FDR cut-off of 0.05 and S0=0.1.[31]

Study approval

All animal procedures were approved by the Institutional Animal Care and Use Committee of the Medical University of South Carolina, protocol number 0488 or the Institutional Animal Care and Use Committee of Emory University, protocol number D-201900225-MOUSE.

RESULTS

Potent antitumor T cells are generated with ex vivo CpG stimulation

We hypothesized that the TLR9 agonist, CpG, could be used ex vivo to augment T cell-based antitumor therapy. To test this idea, we employed the pmel-1 mouse model of ACT in which $CD8^+$ T cells express a transgenic TCR that recognizes the gp100 epitope expressed by melanoma and healthy melanocytes.[32] On day 0, CpG or vehicle (endotoxin-free water) was added to whole pmel-1 splenocytes at the time of TCR stimulation with 1 µM hgp100 peptide. The culture was expanded in the presence of IL-2 for 1 week to preferentially expand pmel-1 $CD8^+$ T cells (henceforth referred to as pmel-1) to >95% purity. After 1 week of expansion, pmel-1 were infused into lymphodepleted mice bearing established B16F10 melanomas (figure 1A). Pmel-1 expanded with CpG were remarkably therapeutic in vivo, as CpG-treated pmel-1 regressed melanoma in mice while vehicle-treated pmel-1 treatment had little therapeutic impact (figure 1B). Mice infused with CpG pmel-1 survived significantly longer than mice given vehicle pmel-1 or mice left untreated (figure 1C). Moreover, pmel-1 engrafted and persisted at higher frequencies in the blood and periphery of mice if they were expanded in the presence of CpG ex vivo (figure 1D,E). Of note, this robust response was achieved without coadministration of IL-2 or vaccine adjuvants in vivo—previously deemed necessary for durable immunity via pmel-1 ACT.[32] We corroborated these findings in another model: a neoantigen TIL therapy model developed by Hanada *et al*.[24] In this model B16F10 cells expressed a modified version of gp100 in which three amino acids of the protein epitope have been replaced making the protein resemble the human version and thus confer higher affinity to the pmel-1 $CD8^+$ T cell receptor when presented on MHC class 1 (online supplemental figure S1A). In this model CpG expanded cells mediated robust and sustained antitumor immunity against large tumors (~100 mm^2) (online supplemental figure S1B). While traditional cell therapy controlled tumors transiently, the tumors eventually relapsed. In contrast, no mice treated with a CpG-expanded $CD8^+$ T cell therapy relapsed and survival was still 100% in this group over 60 days post T cell infusion (online supplemental figure S1C). Thus, adoptively transferred $CD8^+$ T cells can mediate remarkable responses to tumors and robustly persist in vivo when expanded ex vivo with CpG.

In vitro CpG stimulation generates T cells with a unique proteomic signature

As stark differences in antitumor activity were observed in vivo, we hypothesized that CpG treatment leads to the expansion of a $CD8^+$ T cell product phenotypically distinct from conventionally expanded cells. To broadly assess how $CD8^+$ T cells expanded from a CpG-treated culture were different from traditionally expanded cells, we compared these T cell products using proteomic analysis. As portrayed in figure 2A, proteins were extracted, purified and change in protein abundance from CpG treatment were determined using label-free LC-MS/MS-based proteomics of day 7 $CD8^+$ T cells. Not surprisingly, the proteomic profile of vehicle and CpG-expanded $CD8^+$ T cells were clearly divergent based on PCA (figure 2B). Of over 2000 proteins identified between vehicle and CpG-expanded T cells, 77 proteins were significantly different between the 2 groups (Student t-test with permutation-based FDR cut-off of 0.01 and S0=0.1) (figure 2C).

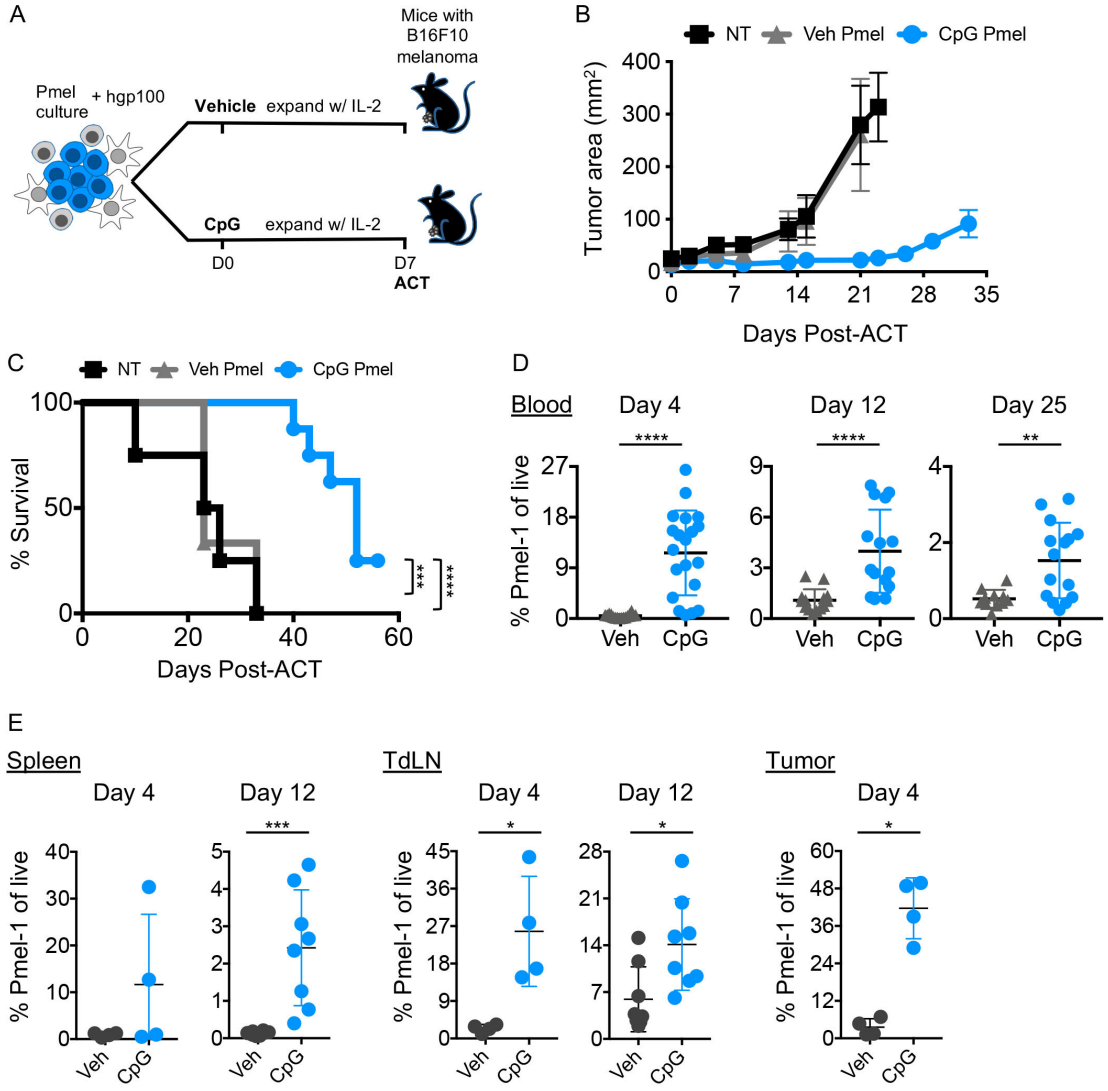

Figure 1 Potent antitumor T cells are generated with ex vivo CpG stimulation. (A) Schema of experimental design. Pmel-1 splenocytes were activated with peptide±CpG on day 0 and expanded in IL-2 until day 7 when they were assayed. Five million pmel-1 CD8$^+$ T cells were infused into mice bearing 5-day established B16F10 melanoma. Mice were irradiated with 5 Gy TBI 1 day prior to cell transfer. (B) Tumor area over time of mice treated with vehicle pmel-1 (n=15), CpG pmel-1 (n=15) or NT (n=6). (C) Survival of mice in (B). (D) Percentage of pmel-1 donor cells in peripheral blood of mice on days 4, 12, and 25 post ACT. (E) Percentage of pmel-1 donor cells in the spleen, tumor-draining lymph node and tumor on days 4 and 12 post transfer. Mice in (E) were infused with 10e^6 vehicle pmel-1 or CpG pmel-1. Statistics: (C) Log-rank test, (D, E) Mann-Whitney U test. **P<0.01, ***p<0.001, ****p<0.0001. ACT, adoptive T cell transfer; IL, interleukin; NT, No Treatment; TBI, total body irradiation; TdLN, tumor-draining lymph node.

Several proteins involved in the processing of fatty acids (ACADLl, ACAD9, CLYBL) and GO molecular functions related to fatty acid oxidation were enriched in CpG-derived pmel-1 (figure 2C,D). There was also a marginally greater population of MitoTracker$^+$TMRM$^+$ pmel-1 TIL in mice treated with a CpG-derived product compared with mice that received a vehicle derived pmel-1 (online supplemental figure S2C). However, the most markedly increased protein in pmel-1 expanded with CpG was IL-2Rα (figure 2C). As IL-2Rα is required to form the high-affinity receptor for the T cell growth factor IL-2, this protein may be important for the antitumor function of CpG-generated T cells.

We validated the expression of IL-2Rα and further investigated the T cell phenotype of CpG pmel-1. We screened more than 20 phenotypic surface markers using flow cytometry to test which proteins were induced in pmel-1 cultures treated with CpG in vitro (online supplemental figure S2A). In agreement with our proteomics analysis, CpG-expanded pmel-1 expressed heightened IL-2Rα (figure 2E). In addition, we found the inducible T cell costimulator (ICOS) was expressed to a higher degree on the surface of CpG-generated CD8$^+$ T cells. IL-2Rα and ICOS have been reported to augment T cell engraftment and function.[33–35] CpG pmel-1 also expressed less CD39, an immunosuppressive ectoenzyme expressed on

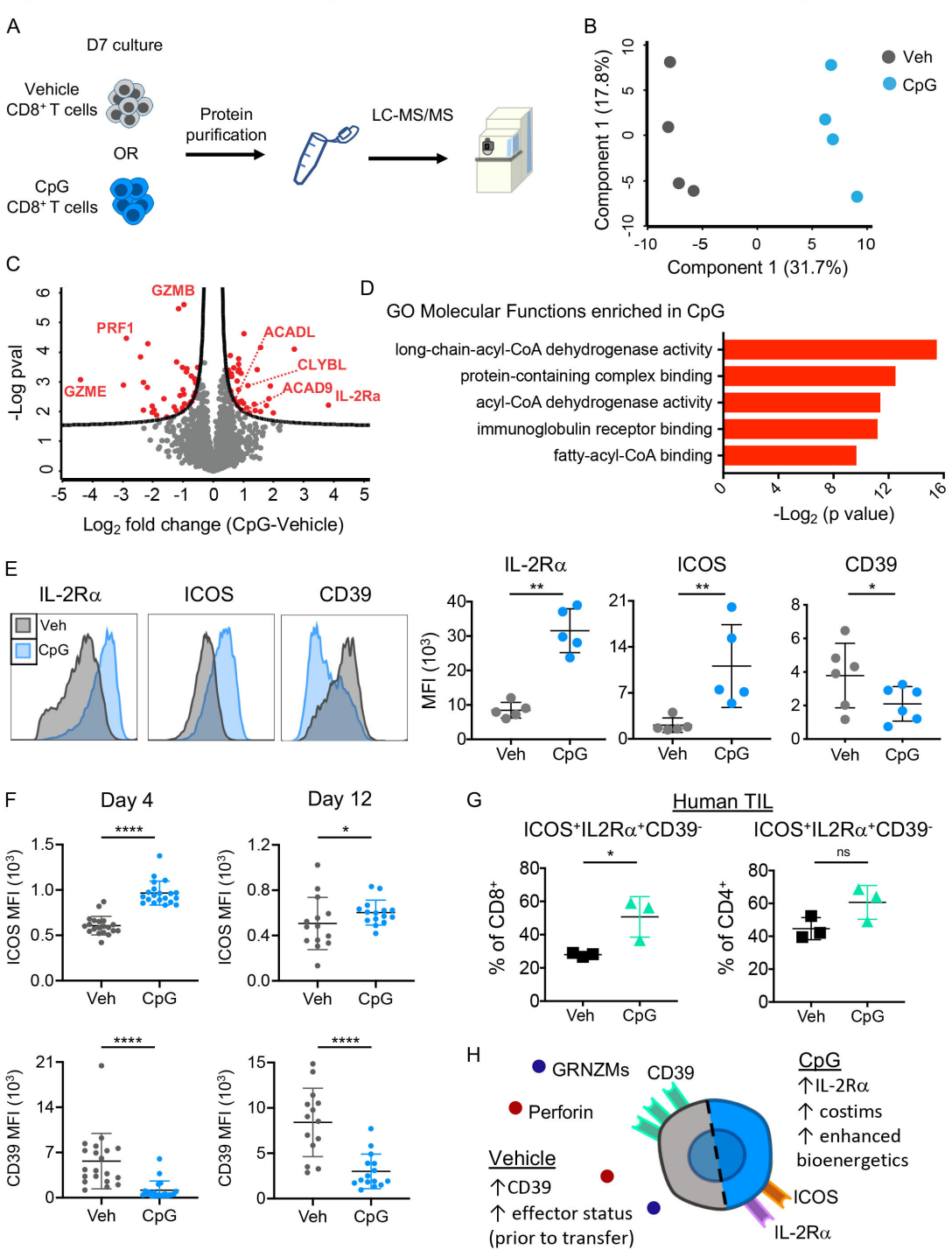

Figure 2 In vitro CpG stimulation generates T cells with a signature phenotype which is maintained post ACT. (A) Design of proteomic analysis of T cells; vehicle or CpG-expanded T cells were collected on day 7 of culture (n=4 mice/group), subjected to protein extraction and purification, and then analyzed using LC-MS/MS. (B) Principle component analysis of vehicle or CpG-generated pmel-1 T cell proteomes. (C) Volcano plot comparing protein expression between vehicle and CpG-expanded T cells. (D) Top 5 GO: molecular functions enriched from proteins expressed more in CpG-generated pmel-1 T cells compared with vehicle-generated cells (using https://toppgene.cchmc.org/enrichment.jsp). (E) Representative flow cytometry histogram (left) and biological replicates (right) of extracellular expression markers from day 7 of cell culture of vehicle or CpG-treated pmel-1. (F) MFI of ICOS (top) or CD39 (bottom) of donor pmel-1 cells in the blood on day 4 or day 12 post ACT. (G) Percentage of human OCSCC TIL expressing IL-2Rα and ICOS, but not CD39 after expansion with CpG. (H) Diagram of CpG-generated T cell characteristics. Statistics: (C) significance threshold was set using two-sided t-test adjusted p value (<0.05 FDR) and a S0 parameter of 0.1. (E) Two-sample t-test, (F) Mann-Whitney U test. *P<0.05, **p<0.01, ***p<0.001, ****p<0.0001. ACT, adoptive T cell transfer; CoA, coenzyme A; FDR, false discovery rate; GO, gene ontology; ICOS, inducible T cell Ccstimulator; IL, interleukin; LC-MS/MS, liquid chromatography-tandem mass spectrometry; MFI, mean fluorescence intensity; ns, not significant; OCSCC, oral cavity squamous cell carcinoma; TBI, total body irradiation; TIL, tumor infiltrating lymphocytes.

exhausted CD8$^+$ T cells,[36 37] than vehicle pmel-1. Thus, when expanded in the presence of CpG, pmel-1 cells display a signature phenotype (IL-2Rα^{high}ICOS^{high}CD39^{low}) (figure 2E). Note, in experiments henceforth, we tracked and used this signature profile as a metric to predict the effect of CpG on pmel-1 CD8$^+$ T cells. Importantly, expression of the signature markers is maintained post ACT as heightened ICOS and diminished CD39 remained characteristic of the CpG-treated donor cells persisting in the peripheral blood as well as the tumor (figure 2F and online supplemental figure S2B). IL-2Rα could not be detected on transferred cells from either group in vivo, possibly due to cytokine binding or rapid receptor cycling from the surface. Further, tumor-infiltrating CpG-generated CD8$^+$ T cells had reduced expression of other markers of suppression or exhaustion including programmed cell death protein 1 (PD-1), lymphocyte activation gene 3 protein (LAG-3), and T cell immunoglobulin and mucin domain-3 (TIM-3), but similar expression of Granzyme B (online supplemental figure S2B). Systemically, inflammatory cytokines including interferon (IFN)-γ and IL-6 were also higher in the plasma of mice that received CpG pmel-1 therapy, indicative of a heightened immune response (online supplemental figure S2D).

To determine if this phenotype would be recapitulated in human cells we cultured TIL from a patient with oral cavity squamous cell carcinoma with human CpG or vehicle at the start of TIL seeding in culture. Similar to their mouse counterparts, both human CD4$^+$ and CD8$^+$ TIL had larger proportions of ICOS$^+$IL2Rα$^+$CD39$^-$ T cells post ex vivo culture with CpG (figure 2G and online supplemental figure S2E). Thus, both mouse and human T cells gain IL-2Rα and ICOS, and lose CD39 after CpG treatment ex vivo (figure 2H). While the functional significance of this signature phenotype on CpG-generated T cell products remained incompletely elucidated, individually each marker has been associated with more or less fit T cells. Thus, we turned our attention to uncovering how addition of CpG to cell cultures could bolster T cell potency.

CpG treatment indirectly alters the CD8$^+$ T cell phenotype and improves tumor immunity

We first questioned whether CpG was directly acting on pmel-1 T cells or if CpG activates other immune cells present at the onset of the culture, imprinting pmel-1 T cells with the signature phenotype and antitumor capacity. Using the online database, ImmGen, we queried *TLR9* expression via available RNA sequencing data sets and found that many B cell, DC, and myeloid subsets express *TLR9* transcripts (online supplemental figure S3A). Conversely, T cell subsets, from both healthy mice and those recently exposed to lymphocytic choriomeningitis virus (LCMV), express trace or undetectable *TLR9* transcripts in the mouse (online supplemental figure S3A). In our mouse model, we corroborated these findings; TLR9 is not expressed in pmel-1 CD8$^+$ T cells but is expressed by professional APCs, which are present only at the start of the TCR-stimulated culture (online supplemental figure S3B). Thus, pmel-1 likely acquire their unique phenotype (IL-2Rα^{high}ICOS^{high}CD39^{low}) after CpG conditioning via TLR9-mediated activation of APCs. The TLR9-expressing APCs in the spleen—B cells, macrophages, and DCs—are present only at the start of culture. These APCs rapidly diminish while CD8$^+$ T cells clonally expand due to peptide-mediated triggering of the pmel-1 TCR. Thus, 3 days after adding peptide to the pmel-1 culture, few APCs remain (not shown).

Using this kinetic information, we designed an experiment to determine whether CpG can act directly on the T cells to confer the signature phenotype and improved tumor immunity. CpG was added at the start of culture on day 0 (early CpG) when APCs and T cells are present, or CpG was added on day 3 (late CpG) when pmel-1 CD8$^+$ T cells dominated the majority of the culture (figure 3A). Pmel-1 CD8$^+$ T cells were assayed for surface IL-2Rα, ICOS, and CD39 1 week after expansion. As anticipated, pmel-1 treated with CpG early expressed high IL-2Rα and ICOS and low CD39 1 week after expansion (figure 3B). Conversely, when CpG was added on day 3 of culture when nominal APCs remained, Late CpG pmel-1 expressed these surface markers to the same extent as vehicle-treated pmel-1 (figure 3B). Early CpG pmel-1 persisted in the blood and tumor and improved therapeutic outcomes and survival (figure 3C-F). However, Late CpG pmel-1 failed to persist in mice and did not improve survival (figure 3D-F).

Our data suggested that either the APCs present at the start of culture or the presence of CpG at priming were critical to the effects it imparted to antitumor CD8$^+$ T cells. Therefore, we performed another experiment to determine if CpG could act directly on pmel-1 in the absence of APCs. Purified pmel-1 CD8$^+$ T cells (negative isolation, >90%) were activated and expanded in the absence or presence of CpG; cells expanded logarithmically as expected (online supplemental figure S4A). As anticipated, purified pmel-1 CD8$^+$ T cells did not gain the signature phenotype or enhanced antitumor efficacy when expanded in the presence of CpG (online supplemental figure S4B,C). Moreover, the engraftment and persistence of enriched pmel-1 T cells treated with CpG were poor (online supplemental figure S4D). Taken together, these findings indicate that CpG does not modulate T cell phenotype directly. Instead, we reasoned that the CpG-mediated effects occur via other APCs present in the culture. Therefore, we questioned whether CpG improved direct or indirect immune cell interactions in the culture to drive the expansion of potent antitumor CD8$^+$ T cells.

Soluble factors are not required for the CpG-improved APC—CD8$^+$ T cell interaction

Specific cytokines secreted by innate immune cells in culture can skew T cell phenotypes. The phenotype we observed in our CpG-treated cells recapitulated,

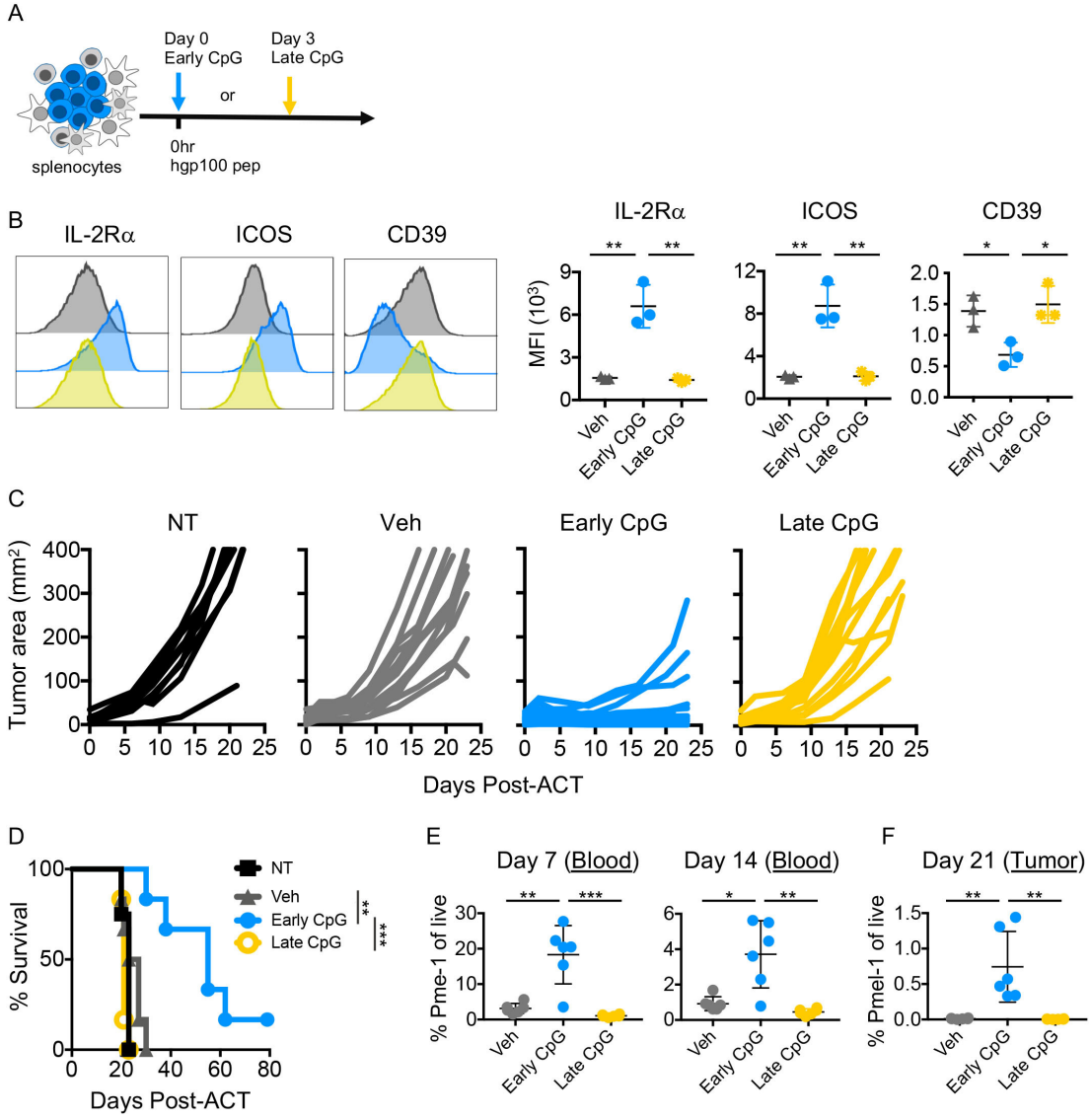

Figure 3 CpG treatment indirectly alters the CD8⁺ T cell phenotype and improves tumor immunity. (A) Schema of experimental design; pmel-1 splenocytes were treated with CpG at the time of activation (early) or 3 days post activation (late) with peptide or treated with vehicle at the time of activation. (B) Phenotypic marker expression on day 7 of culture (n=3 biological replicates). (C) Tumor area over time (single curves represent one mouse) treated with NT, vehicle pmel-1, early CpG pmel-1, or late CpG pmel-1. Single curves are combined from two individual experiments; n=9–12 mice/group. (D) Survival of mice in (C). (E) Percentage of donor cells in the blood of mice from (C) on day 7 and day 14 post ACT. (F) Percentage of donor cells in the tumor of mice treated in (C) on day 21 post ACT. Statistics: (B) Two-sample t-test. (D) Log-rank test. (E, F) Mann-Whitney U test *p<0.05, **p<0.01, ***p<0.001, ****p<0.0001. ACT, adoptive T cell transfer; ICOS, Inducible T Cell Costimulator; IL, interleukin; MFI, Mean Fluorescence Intensity; NT, No Treatment.

in part, a report of pmel-1 conditioned with IL-12.[38] Thus, we hypothesized that CpG treatment induced the secretion of pro-inflammatory cytokines and chemokines in the culture by TLR9 expressing immune cells and that these soluble factors were responsible for promoting the pmel-1 CD8⁺ T cell phenotype, IL-2Rα^{high}ICOS^{high}CD39^{low}.

To first get a broad idea of the soluble factors induced post-CpG treatment, we collected and froze supernatant at 48 hours after treatment with CpG or vehicle. Supernatant was analyzed for the presence of 44 chemokines and cytokines via a multiplex array (Eve Technologies). Many cytokines and chemokines were increased in the supernatant of CpG-treated cultures on day 2 post treatment compared with vehicle treated cells (online supplemental figure S5A,B). To determine if the most abundant factors were responsible for skewing the CpG-associated phenotype, we blocked the top hits associated with CpG. We individually targeted the top five proteins from our array, which included IFN-γ, IL-6, TIMP-1, CXCL10, and IL-10, during cell culture. Each blocking antibody (or isotype control) was added immediately prior to the addition of hgp100 peptide and vehicle or CpG on day 0 and daily thereafter for the duration of culture. To our surprise, CpG-generated CD8⁺ T cells retained their IL-2Rα^{high}ICOS^{high}CD39^{low} phenotype independent of

blockade of any of these targets, suggesting that these soluble factors were not required for the effects of CpG on T cells (online supplemental figure S5C). As mentioned previously, some of our phenotype was similar to that of IL-12 conditioned T cells, thus we tested IL-12 blockade as well, but this cytokine was also dispensable for the signature phenotype (not shown).

However, in criticizing our approach to this question, we noted that perhaps individual cytokines and chemokines might be insufficient to drive CpG-mediated effects on donor antitumor $CD8^+$ T cells. Instead, we hypothesized that a collection of these factors, in the supernatant of CpG-treated cultures, were causing the acquisition of the signature phenotype. Thus, we next performed a supernatant transfer experiment. For this experiment, we froze supernatant from CpG or vehicle treated bulk pmel-1 splenocytes at 7 and 48 hours post activation with hgp100 peptide. Stored supernatant was then used to stimulate fresh bulk pmel-1 splenocytes or $CD8^+$ isolated pmel-1 T cells. As controls, we also stimulated bulk pmel-1 splenocytes or $CD8^+$ isolated pmel-1 T cells directly with CpG or vehicle to ensure that CpG had the typical effect on the pmel-1 $CD8^+$ T cells generated from a bulk culture (online supplemental figure S5D). Each group was then grown for 7 days in culture and assayed for surface phenotypic markers. We suspected that bulk pmel-1 splenocytes treated directly with CpG would generate $CD8^+$ T cells with the IL-2Rα^{high}ICOS^{high}CD39^{low} phenotype while CD8 purified T cells would not acquire this phenotype when treated with CpG. Similarly, we thought that supernatant collected at the early time point from the culture (7 hours), when CpG is likely still available, would confer the phenotypic alterations when transferred to bulk pmel-1. However, we posited that supernatant collected at a later time (48 hours) from CpG-treated cultures, would likely be depleted of CpG and thus not induce the typical changes to $CD8^+$ T cells derived from bulk pmel-1 cultures. In contrast to when CpG is added directly to purified T cells, we thought that transferring supernatant from CpG-treated cultures, which is rich in cytokines and chemokines would expand $CD8^+$ T cells with the IL-2Rα^{high}ICOS^{high}CD39^{low} phenotype. $CD8^+$ pmel-1 T cells from bulk splenocytes acquired the CpG associated phenotype after transfer of CpG-supernatant that was collected at the early time point (7 hours), but not the late time point (48 hours). However, no supernatant transfer conditions reproduced the signature phenotype on purified $CD8^+$ T cells (online supplemental figure S5E). Additionally, supernatant from vehicle treated cultures did not induce IL-2Rα^{high}ICOS^{high}CD39^{low} $CD8^+$ T cells under any conditions (online supplemental figure S5E). This finding indicates that cytokines and chemokines secreted as a result of CpG treatment do not support the generation of $CD8^+$ T cells with high expression of IL-2Rα and ICOS and low expression of CD39, suggesting the CpG facilitated interaction between T cells and APCs in culture is not mediated by a soluble factor.

A direct interaction between T cells and APCs is critical for the CpG induced effects

As secreted factors did not appear to foster the CpG-associated phenotype in antitumor T cells, we hypothesized the direct interaction between APCs and pmel-1 T cells in culture was required. Initially, we tested this idea by blocking a costimulatory pair critical for bolstering B and $CD4^+$ T cell interactions: the CD40/CD40L pathway. However, blocking this pathway did not impact the outgrowth of $CD8^+$ T cells with the CpG signature phenotype nor did it hinder their in vivo potency (online supplemental figure S6A-C). Thus, we next tested this 'interface' idea using a series of experiments designed to bypass the direct interaction between T cells and APCs during antigen presentation. Specifically, we activated pmel-1 cultures with one of the following strategies: (1) hgp100 peptide (positive control—mediates B–T cell communication via MHC-I-TCR signaling), (2) plate-bound anti-CD3 (bypasses MHC-I-TCR signaling), (3) plate-bound anti-CD3/anti-CD28 (bypasses MHC-I-TCR signaling), or (4) bead-bound anti-CD3/anti-CD28 (bypasses MHC-I-TCR interactions) in the presence or absence of CpG (figure 4A). After 7 days of expansion, pmel-1 cells activated with any strategy that bypassed the use of an APC, did not acquire the same phenotype as those activated via APCs and hgp100 peptide when in the presence of CpG (IL-2Rα^{high}ICOS^{high}CD39^{low}). Instead, when plate-bound or bead-bound antibodies were used in place of peptide activation, the phenotype was similar between vehicle and CpG-expanded T cells (figure 4B-C and online supplemental figure S7A).

Based on this finding, we questioned if bypassing the APC in vitro would also abrogate the in vivo antitumor efficacy of CpG-generated T cells. Indeed, we found that the antitumor efficacy gained with CpG treatment of peptide activated cells was not recapitulated when CpG was used alongside CD3/CD28 beads, plate-bound CD3/CD28 or plate-bound anti-CD3 activation (figure 4D and online supplemental figure S7B). Mice that received cell therapies derived from any strategy in which the MHC-I-TCR interaction was bypassed had significantly reduced survival compared with those who received T cells that were activated with peptide and CpG (figure 4E and online supplemental figure S7C). Though the engraftment and persistence of the donor T cells were bolstered in mice which received the peptide/CpG stimulated culture product, neither metric was enhanced in mice that received a product generated in the presence of CpG when the APCs were bypassed (figure 4F). Together, these findings indicate an intimate, direct, interaction between APCs and T cells in CpG-treated cultures drive the expansion of potent $CD8^+$ T cells.

The phenotype of CpG-generated $CD8^+$ T cells is largely dependent on B cells

While many different immune cells are present in the early stages of $CD8^+$ TIL cultures, intracellular TLR9 expression is limited to B cells, DCs, and macrophages

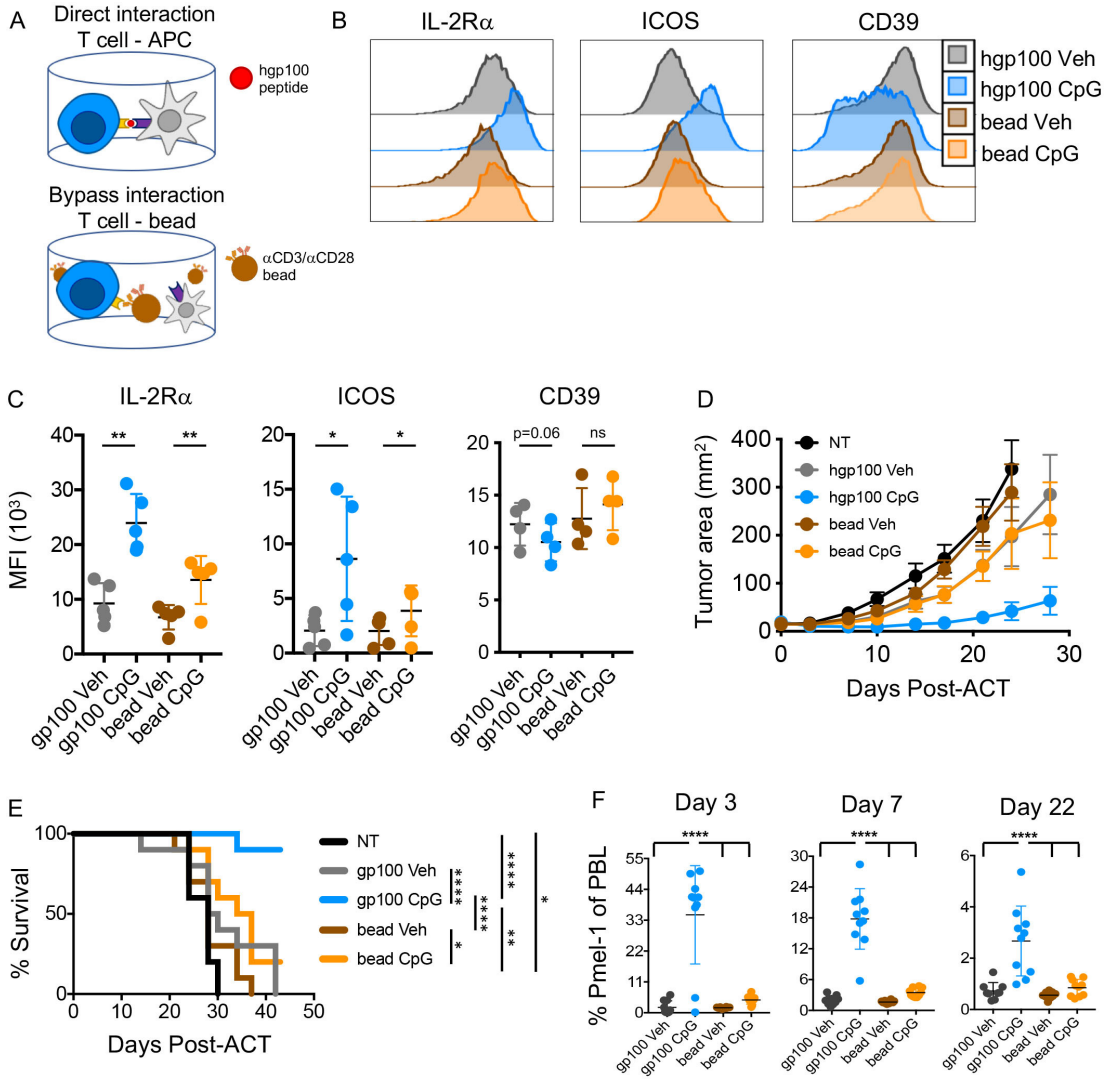

Figure 4 Direct interaction between CD8⁺ T cells and APCs is required for the CpG-mediated effects. (A) Schematic of hgp100 peptide mediated activation via MHC-I—pmel-1 TCR vs bypassing the APC using bead-bound αCD3/αCD28 agonistic antibodies. (B) Representative histograms of signature phenotypic marker expression on CD8⁺ pmel-1 T cells expanded from cultures activated via APCs (hgp100 peptide) or when APCs were bypassed (αCD3/αCD28 beads). (C) Biological replicates of signature phenotypic marker expression on groups from (B). (D) Tumor area over time of mice treated with CD8⁺ pmel-1 T cells expanded from vehicle or CpG-treated cultures activated with hgp100 peptide or αCD3/αCD28 beads. (E) Survival of mice in (D). (F) Percentage of donor cells in the blood of mice treated in day at 3, 7, and 22 days post ACT. Statistics: (C) Two-sample t-test. (E) Log-rank test. (F) Ordinary one-way analysis of variance with Tukey's multiple comparison test, at each collection time point *P<0.05, **p<0.01, ***p<0.001, ****p<0.0001. ACT, adoptive T cell transfer; APC, antigen-presenting cell; ICOS, Inducible T Cell Costimulator; IL, interleukin; MFI, Mean Fluorescence Intensity; MHC, Major Histocompatibility Complex; NT, No Treatment; PBL, Peripheral Blood Leukocytes.

in the mouse (online supplemental figure S3B). Thus, we next sought to identify which APC was important for generating pmel-1 with the signature phenotype associated with CpG-promoted tumor immunity. We hypothesized that DCs were critical, as they are potent TLR9⁺ APCs that secrete cytokines and express heightened MHC I and II molecules when activated with CpG.[39–42] To address this question, B cells, DCs, or macrophages were individually depleted or DCs and macrophages were dually depleted from the starting cell culture prior to expansion for 7 days and phenotypic analysis. As additional controls, we also removed CD4⁺ T cells or NK cells before the start of culture as these populations are also present in pmel-1 splenocytes. In contrast to our hypothesis, depleting DCs from the CpG-treated cell culture did not hinder the outgrowth of pmel-1 with the signature phenotype. Instead, only B cell depletion prevented the expansion of IL2Rα^{high}ICOS^{high}CD39^{low} pmel-1 CD8⁺ T cells (figure 5A). Indeed, whether macrophages, CD4⁺ T cells, or NK cells were depleted, CpG treatment could still propagate IL2Rα^{high}ICOS^{high}CD39^{low} pmel-1 cells (figure 5A and online supplemental figure S8B). Dual depletion of DCs and macrophages did not disrupt the

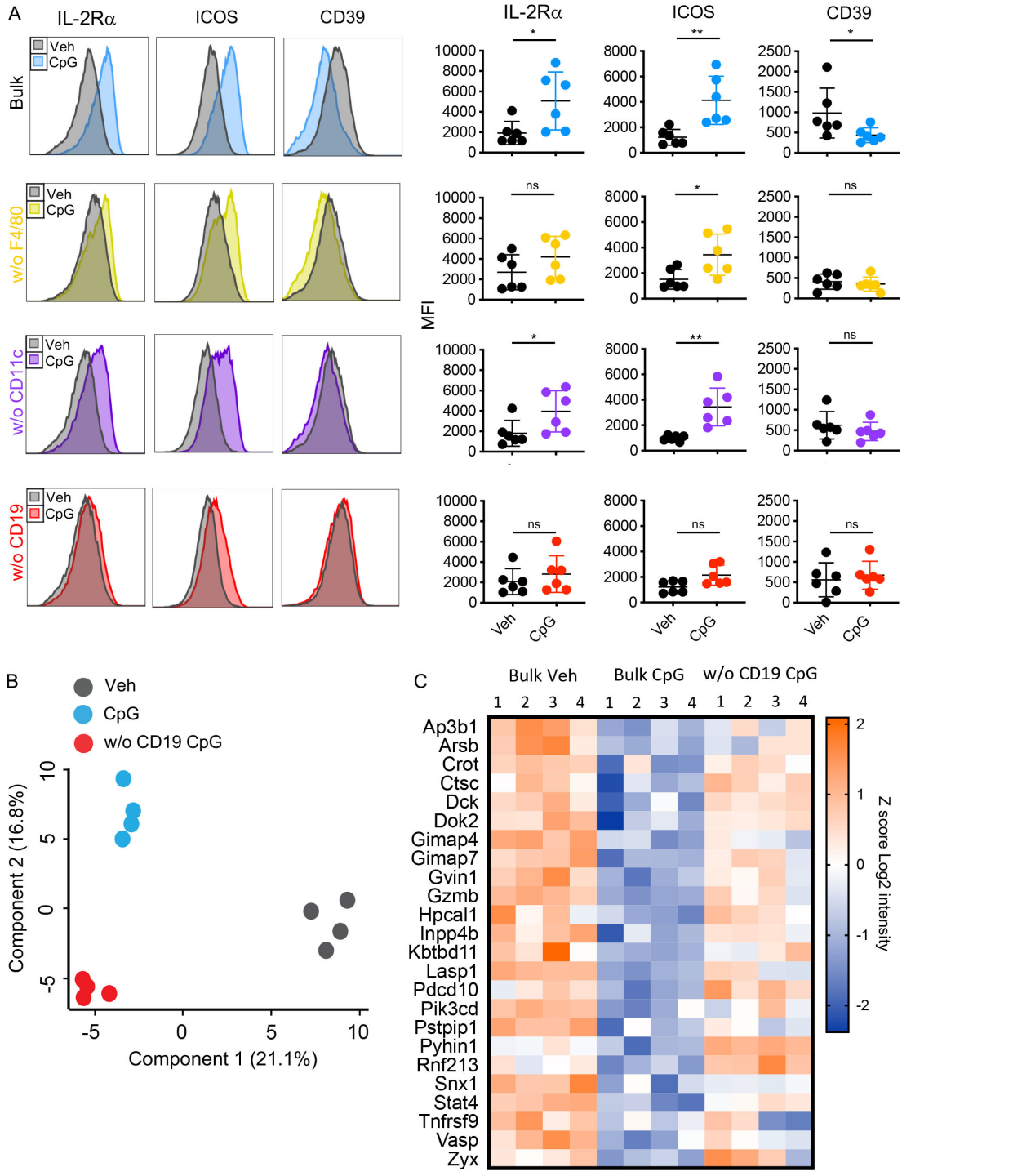

Figure 5 The phenotype of CpG-generated CD8⁺ T cells is largely dependent on B cells. (A) Histograms (left) and biological replicates (n=6) (right) of the expression of signature phenotype markers on the cell surface on day 7. T cells were expanded from bulk, F4/80-depleted, CD11c-depleted, or CD19-depleted cell cultures treated with vehicle control or CpG. (B) Principle component analysis of proteomic signatures of day 7 expanded T cells derived from a bulk vehicle or CpG-treated culture, or a CD19-depleted CpG-treated culture (n=4 biological replicates). (C) Heatmap comparing Z scores (of the Log2 protein intensity value) from the T cells expanded from the same groups as in (B). Displayed are proteins that were expressed significantly higher (determined using two-sided t-test adjusted p value (false discovery rate <0.05) and an S0 parameter of 0.1) in bulk vehicle generated T cells compared with bulk CpG-generated T cells. Statistics: (A) Mann-Whitney U test.*P<0.05, **p<0.01. ICOS, Inducible T Cell Costimulator; IL, interleukin; MFI, Mean Fluorescence Intensity; ns, not significant; SCR, scramble ODN.

acquisition of the IL2Rα^{high}ICOS^{high}CD39^{low} phenotype with CpG expansion (online supplemental figure S8F).

To examine global changes in CpG-expanded pmel-1 on depletion of B cells, we used proteomics to determine specific characteristics of CpG-expanded T cells in the presence or absence of B cells. We included traditionally-expanded T cells (bulk vehicle) as a control to see whether removing B cells essentially reverts the phenotypic effects of CpG to that of a vehicle-derived population. By PCA, the ACT products (vehicle, CpG-expanded, or CpG-expanded CD19 depletion) did not overlap, indicating that each of these groups was distinctly different from one another at the proteomic level (figure 5B). We next tested if depleting B cells results in the expansion of a cell product that more closely resembles the ineffective vehicle-derived CD8$^+$ T cells. We found that a majority of the proteins which were significantly enriched in vehicle-expanded pmel-1 were also more abundant in CD19-depleted CpG-treated cells compared with T cells expanded from a bulk culture treated with CpG (figure 5C). Under certain circumstances, several of these proteins that were abundant in both the bulk vehicle and CD19-depleted CpG expanded pmel-1 have been associated with highly activated or terminally exhausted T cells including: GZMB, TNFRSF9, and PIK3CD.[43 44] However, these same proteins can also promote activation, costimulation, and cytotoxic function of T cells. These results indicate that CD19$^+$ B cells, in the context of CpG, drive broad phenotypic alterations in T cell products, but do not reveal whether B cells are critical for the potent tumor immunity seen after expansion with CpG.

Removal of B cells from the culture ablates the improved antitumor efficacy with CpG

Since B cells were critical to the CpG-mediated phenotypic impact on CD8$^+$ T cells, we hypothesized that B cells would be similarly critical for the antitumor activity of CpG-expanded pmel-1. To test this idea, we depleted B cells, CD11c$^+$ DCs, F4/80$^+$ macrophages, CD4$^+$ T cells or NK1.1$^+$ NK cells from the starting culture. These cultures were then peptide activated with or without the addition of CpG, expanded and adoptively transferred into tumor-bearing mice (figure 6 and online supplemental figure S8). We found that when B cells were removed from the culture, CpG pmel-1 cells were as ineffective as vehicle pmel-1 cells at regressing tumors in vivo (figure 6A). Conversely, when DCs, macrophages, CD4$^+$ T cells, or NK cells were individually depleted, the therapeutic efficacy of CD8$^+$ T cells with CpG treatment was maintained (figure 6A and online supplemental figure S8C). We also depleted DCs and macrophages concomitantly and found that CpG expanded cells still improved the survival of mice (online supplemental figure S8G). No survival advantage was achieved in mice treated with CpG pmel-1 that were expanded in the absence of B cells ex vivo (figure 6B). Engraftment and persistence of pmel-1 in the blood were improved if cultures were treated with CpG, even in the absence of DCs, macrophages, NK or CD4$^+$ T cells, at the start of culture (figure 6C and online supplemental figure S8E). In contrast, the engraftment and persistence of CpG-treated pmel-1 cultures depleted of B cells were poor (figure 6C). These findings uncover a key role for TLR9-activated B cells in generating CD8$^+$ T cells with potent antitumor immunity.

B cells alone are sufficient to improve antitumor T cells after activation via TLR9

We assumed purified B cells could enhance pmel-1 CD8$^+$ T cells for ACT via CpG activation of TLR9, but it remained unknown if the same extent of tumor immunity would be mediated if B cells were the sole APC. Thus, we examined the signature phenotype and antitumor properties of CpG-generated cells in bulk and purified B cell/T cell co-cultures. As seen in bulk cultures treated with CpG, when CD8$^+$ T cells were expanded from a co-culture of CD8$^+$ T cells and B cells treated with CpG, T cells also expressed more IL2Rα and ICOS. CD39 expression was similar between both CpG and vehicle treated groups in the purified B plus T cell co-culture, but the overall expression of both groups was lower than that of vehicle T cells generated from a bulk culture (figure 7A and online supplemental figure S9A). Mice given either of the CpG-derived pmel-1 products arrested tumor outgrowth and enhanced survival time compared with mice treated with vehicle cells or those that were not treated (figure 7B–D). Survival did not differ between the two CpG-treatment groups, suggesting that B cells are sufficient to induce the potency of pmel-1 CD8$^+$ T cells via CpG. Of note, pmel-1 generated without CpG, but from a B and T cell co-culture, were more effective antitumor T cells than their bulk vehicle counterparts, as demonstrated by both the slower outgrowth of tumors and longer survival (figure 7B–D). There was no significant difference in tumor control or survival in mice given the bulk CpG-treated product over those given the pure B/T cell CpG-treated product (figure 7B–D). Also, mice treated with either CpG-generated cell product had more donor pmel-1 cells in their blood 1 week after infusion, indicating better engraftment of CpG-generated T cells (figure 7E).

Collectively, we found that a highly effective CD8$^+$ T cell product can be achieved by simply adding the TLR9 agonist, CpG, to cell expansion protocols. Moreover, the mechanism of action of CpG is mediated by B cells, and B cells alone are sufficient to promote this powerful antitumor T cell product via CpG.

DISCUSSION

Herein we describe a novel use for a microbial ligand, the synthetic TLR9 agonist CpG DNA, for adoptive cellular therapy. We reveal CpG can be added to the ex vivo cell expansion process to reverse the tolerant state of CD8$^+$ T cells to tumors in vivo and augment cancer treatment. Perhaps most surprizing, B cells were essential to the manifestation of this potent T cell product as

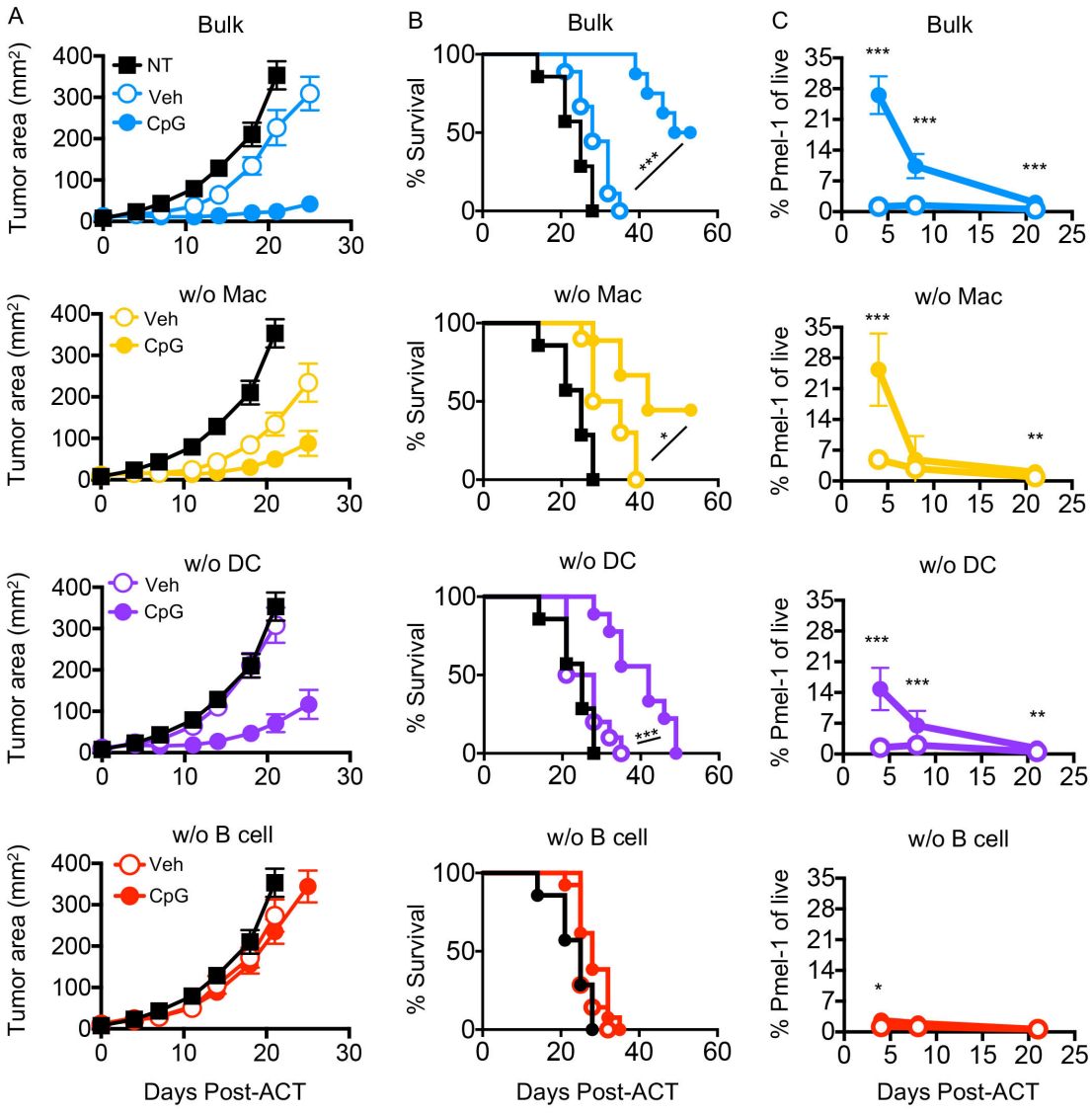

Figure 6 Removal of B cells from the culture ablates improved antitumor efficacy with CpG. (A) Tumor area over time of mice treated with NT, or vehicle or CpG-generated T cell products from bulk, macrophage, DC, or B cell-depleted cultures (n=7–13 mice/group). Bulk indicates the T cell product was grown out of a whole splenocyte mixture seeded on day 0 while in 'depleted' cultures the T cell infusate was derived from a culture depleted of individual subsets on day 0. (B) Survival of mice in (A). (C) Percentage of donor cells in the blood of mice treated in (A) on day 4, day 8, and day 211 post ACT. Statistics: (B) Log-rank test. (C) Mann-Whitney U test at each time point. *P<0.05, **p<0.01, ***p<0.001, ****p<0.0001. ACT, adoptive T cell transfer; DC, dendritic cell; NT, No Treatment.

observed through our cell depletion and purified co-culture studies.

The properties that drive CpG-generated T cells to robust antitumor responses in vivo are still unclear. Given our finding that CpG-induced T cells increase IL-2Rα and ICOS expression but express less CD39, a natural question follows: Do these molecules influence the potency of antitumor T cells? Our team previously reported that IL-2Rα on activated T cells allows them to respond in an improved and temporal fashion to IL-2, in vivo, and mediate antitumor immunity.[33] Further overexpression of IL-2Rα improves T cell tumor control.[24] ICOS, which is also highly elevated on CpG-treated pmel-1 T cells, supports the function and antitumor activity of various types of cell products, including TIL and antigen receptor (CAR or TCR) therapies.[34 35] ICOS signaling on T cells is also crucial for an antitumor response post-CTLA4 blockade, Th17 and Tc17 therapies.[34 35 45] Finally, CpG-mediated downregulation of the ectoenzyme CD39 may improve T cell tumor immunity. As CD39 is a key enzyme in the catabolism of pro-inflammatory adenosine triphosphate (ATP) to immunosuppressive adenosine, a diminishment of CD39 may lead to less inhibitory adenosine within the tumor.[46] Moreover, CD39 marks effector T cells that have an exhausted phenotype in patients with infectious disease and cancer and have reduced survival after activation in older individuals.[36 37 47] In patients with metastatic melanoma, Krishna *et al* demonstrated that CD39 and CD69 expression can be used to bifurcate patient response to cell therapy and that some CD39⁻ TIL from

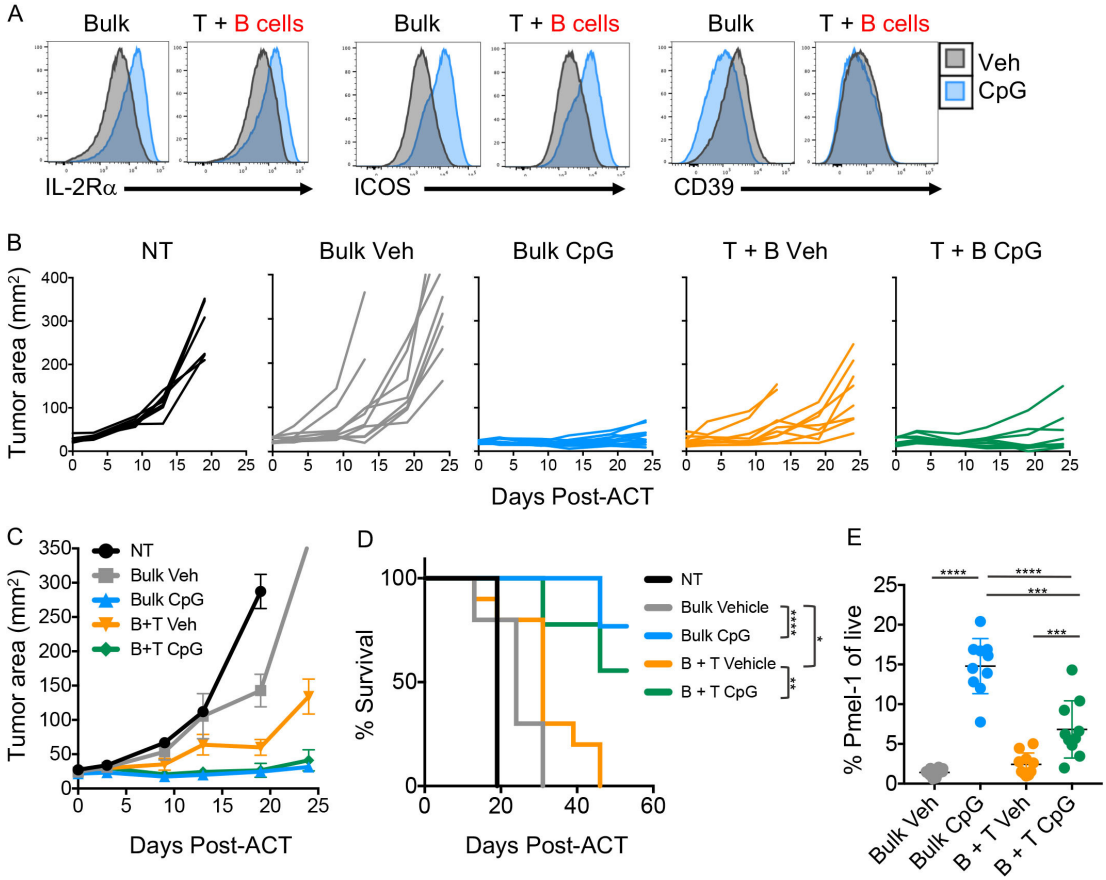

Figure 7 B cells alone are sufficient to improve antitumor T cells after activation via TLR9. (A) Phenotype of day 7 T cells. (B) Tumor area over time (single curves represent one mouse) of mice treated with NT, bulk vehicle pmel-1, bulk CpG pmel-1, B+T vehicle pmel-1, or B+T CpG pmel-1 (n=8–13 mice/group). Bulk indicates the T cell product was grown out of a whole splenocyte mixture seeded on day 0 while B+T indicates the T cell infusate was derived from a culture of purified B cells co-cultured with purified T cells seeded on day 0. (C) Average tumor area over time of mice treated in (B). (D) Survival of mice in (B). (E) Percentage of donor cells (Vβ13$^+$CD8$^+$) in peripheral blood of mice treated with each group listed in (B) on day 7 post ACT. Statistics: (D) Log-rank test. (E) Mann-Whitney U test, *p<0.05, **p<0.01, ***p<0.001, ****p<0.0001. ACT, adoptive T cell transfer; TLR, Tool-like receptor; ICOS, Inducible T Cell Costimulator; NT, No Treatment.

these patients are neoantigen recognizing stem-like T cells, which are known to potentiate powerful antitumor responses.[48] Thus, it is likely that the reduced CD39 and overt expression of IL-2Rα and ICOS on T cells post CpG treatment potentiate T cell function, metabolism, and persistence in vivo. Critically, this phenotype was shared by human TIL, both CD4$^+$ and CD8$^+$ T cells, that were expanded in the presence of CpG. The contribution of these surface molecules (separately or in combination) on the efficacy of this therapy will be explored in future studies.

Our proteomic screen of T cell products points also to increased fatty acid oxidation (FAO) in CpG-expanded cultures compared with traditionally-expanded T cells. Several reports demonstrate FAO is important for the development of memory T cells and their enhanced survival.[49–51] As CpG-derived T cells survive far longer in vivo compared with vehicle-derived T cells, this advantage may in part be due to enhanced mitrochondrial FAO-based energetics. In the tumor, there was a marginally greater population of MitoTracker$^+$TMRM$^+$ pmel-1 TIL in mice that received CD8$^+$ T cells from a CpG-treated culture compared with a vehicle-treated culture. However, further investigation is required to determine how CpG indirectly modulates T cell metabolism and if it plays a role in the effectiveness of this cellular therapy.

Using two experimental approaches, one in which CpG was added to purified T cells and one in which CpG was added when few APCs remained in culture, we discovered that CpG does not directly alter the CD8$^+$ T cell phenotype or antitumor ability via TLR9 signaling. This finding was not surprizing as CD8$^+$ T cells express nominal TLR9.

Instead, we found that B cells in the CpG-treated culture were most vital for enhancing the antitumor potency of T cells for ACT. This finding is illuminated by our discovery that CpG-generated cells were completely ineffective in vivo when B cells were removed from the culture. In contrast, the CpG product remained effective against melanoma when F4/80$^+$ macrophages, CD4$^+$ T cells or NK1.1$^+$ NK cells were removed from the culture. Likewise, removing CD11c$^+$ DCs (with or without F4/80$^+$ macrophages), did not impair the antitumor potency

of CpG-treated pmel-1 T cells. It should be appreciated however that various DC subsets, such as myeloid and plasmacytoid DCs (pDCs), can differentially impact tumor immunity. In our experiments, we removed CD11c$^+$ DCs, yet, pDCs express intermediate levels of CD11c, so this subset may not have been completely removed from our T cell product. As pDCs express high TLR9, follow-up experiments may shed light on the specific role of pDCs in CpG-conditioned ACT products. Most notably, however, when bulk B cells were depleted by targeting CD19, the antitumor potency of CpG-T cells was completely lost. However, B cell subsets, such as marginal zone and follicular B cells, respond differently to TLR9 stimulation and impact T cell immunity in distinct ways.[39] Thus, further investigations are warranted to determine if a specific B cell subset is uniquely positioned to empower CD8$^+$ T cells with robust antitumor activity via CpG.

What remained striking to us was the ability of TLR-activated B cells to foster the development of potent antitumor CD8$^+$ T cells for ACT. However, depleting B cells from the cell culture did not satisfy the question of whether B cells alone were able to generate this T cell product via CpG. This distinct question is of critical importance, as the translation of this finding would be more feasible if isolated B cells could impart this biology on T cells via CpG without the need for other immune cells. When purified B and CD8$^+$ T cells were co-cultured, the addition of CpG improved their activity when infused into mice with large tumors. Of note, B cells slightly enhanced CD8$^+$ T cell immunity even when CpG was not present. This work further underscores that B cells could be considered in the manufacturing of T cell products for adoptive immunotherapy.

The finding that B cells were critical for the efficacy of CpG-improved T cell therapy leads to several questions of the mechanism of these cells' interaction. Studies herein reveal that the potency of this therapy is reliant on a contact dependent CpG-promoted B cell/T cell interaction mediated by MHC-I-peptide-TCR signaling, as bypassing this crosstalk using αCD3/αCD28 beads (or plate-bound antibodies) abrogated the CpG-induced benefit to treatment. In contrast, CpG facilitated the B–T cell crosstalk via MHC-I-TCR signaling via tumor antigen (hgp100) peptide. This CpG induced interaction was needed to potentiate the phenotype of antitumor CD8$^+$ T cells, and in turn enhance their capacity to regress and even ablate tumors in vivo. Interestingly, we found that although CpG induced many inflammatory factors in our cultures, they were not the main contributors to the CpG augmentation of T cell products. Follow-up studies will be required to more intimately understand how CpG empowers B–T cell interactions to direct the fate, function, and antitumor activity of adoptively transferred CD8$^+$ T cells in immunotherapy.

B cells are emerging as a potentially critical presence in successful immunotherapies. In fact, several exciting studies have revealed that the presence of B cells in tertiary lymphoid structures in multiple malignancies served as a powerful prognostic indicator of successful immune checkpoint blockade (ICB) therapies.[52–54] Several features unique to ICB responders arose: the presence of specific B cells subsets, altered B cell receptor (BCR) clonality and diversity, and B cell/T cell interactions within the tumor microenvironment (TME). However, whether or how each of these observations drive response to checkpoint blockade and if their presence is predictive of response to ICB in other malignancies remains to be determined. As B cells can play multiple roles in the immune response—antibody production to tumor antigens, presentation of antigens to CD4$^+$ and CD8$^+$ T cells, and cytokine/chemokine production—it is likely that they contribute to tumor immunity in vivo in a number of ways. Indeed, tumor-infiltrating B cells (TIL-B) have been shown to act as APCs ex vivo to CD4$^+$ TIL from human non-small cell lung cancer tumors.[55] Thus, exploiting and enhancing this interaction by incorporating TLR agonists, is a logical future direction. The findings from these clinical reports alongside our findings prompt another question of whether B cells, in vivo, are also critical for the response of adoptive T cell therapies for cancer.

Our findings can be directly translated to improve cell therapies. In TIL-based ACT therapies, two approaches could be used: (1) at the onset of culture when tumor pieces harbor a TIL-B population or (2) during rapid expansion in which T cells are expanded in the presence of peripheral blood mononuclear cell (PBMC) feeder cells to large numbers before returned to the patient. We posit that incorporating CpG into either step of ex vivo expansion could lead to improved cellular therapies. Importantly, B cell populations vary widely among tumors, so strategies to exploit them in an ex vivo TIL culture may depend on the starting number and phenotype. One-way to account for this variability could be to supplement TIL cultures with B cells from the peripheral blood or tumor draining lymph nodes. Ongoing studies in our laboratory seek to understand how to best use CpG in clinical trials at various institutions. Collectively, our work demonstrates, for the first time, the importance of B cells in generating potent CD8$^+$ T cell products for cancer immunotherapy.

Author affiliations
[1]Department of Microbiology and Immunology, Medical University of South Carolina, Charleston, South Carolina, USA
[2]Division of Surgical Oncology, Department of Surgery, Emory University, Atlanta, Georgia, USA
[3]Department of Microbiology and Immunology, Winship Cancer Institute, Emory University, Atlanta, Georgia, USA
[4]Department of Otolaryngology—Head and Neck Surgery, Medical University of South Carolina, Charleston, South Carolina, USA
[5]Department of Cell and Molecular Pharmacology and Developmental Therapeutics, Medical University of South Carolina, Charleston, South Carolina, USA
[6]Division of Medical Oncology, The Ohio State University, Columbus, Ohio, USA
[7]Division of Hematology, Department of Internal Medicine, The Ohio State University, Columbus, Ohio, USA
[8]Department of Cell Biology & Physiology, University of North Carolina at Chapel Hill, Chapel Hill, NC, USA
[9]Immunotherapy Program, Lineberger Comprehensive Cancer Center, University of North Carolina at Chapel Hill, Chapel Hill, NC, USA

[10]Department of Internal Medicine, Division of Molecular Medicine, University of New Mexico Health Sciences Center, Albuquerque, New Mexico, USA

Twitter Aubrey S Smith @Aubrey_Smith04 and Chrystal M Paulos @PaulosLab

Acknowledgements We would like to acknowledge several individuals from the Mass Spectrometry Facility, a University Research Resource at MUSC, specifically: Susana Comte-Walters, Jennifer R Bethard, Baylye Burnette, and Lauren Ball for their assistance with our proteomic analyses. Proteomic analysis was performed at the Mass Spectrometry Facility, a University Shared Research Resource at the Medical University of South Carolina, using instrumentation acquired through the NIH shared instrumentation grant program (S10 OD010731-Orbitrap Elite Mass Spectrometer or Orbitrap Fusion Lumos ETD/UVD MS (S10 OD025126). This work was supported in part by the Cell Evaluation and Therapy Shared Resource, Hollings Cancer Center, Medical University of South Carolina (P30 CA138313). Research reported in this publication was supported in part by the Pediatrics/Winship Flow Cytometry Core of Winship Cancer Institute of Emory University, Children's Healthcare of Atlanta and NIH/NCI under award number P30CA138292. The content is solely the responsibility of the authors and does not necessarily represent the official views of the National Institutes of Health. We thank Kent Armeson for his guidance on statistical analyses. We thank our collaborators for their valuable feedback: Arman Aksoy, Pinar Aksoy, Elinor Gottschalk, Dimitrios Arhontoulis, Stephen Iwanowycz, Katie Hurst, Gregory Lesinski, Ragini Kudchadkar, David Lawson and Melinda Yushack.

Contributors ASS: Conceptualization, data curation, formal analysis, investigation, methodology, visualization, writing—original draft, writing—review and editing. HMK: Data curation, investigation, validation, writing—review and editing. MMW: Conceptualization, data curation, investigation, methodology, supervision, writing—review and editing. GORR: Data curation, investigation, writing—review and editing. AMR-R: Data curation, investigation, writing—review and editing. CJD: Data curation, investigation, writing—review and editing. MBW: Data curation, investigation, writing—review and editing. ACC: Data curation, investigation, writing—review and editing. DMN: Resources, supervision, writing—review and editing. JET: Investigation, methodology, resources, supervision, writing—review and editing. EB: Investigation, methodology, supervision, writing—review and editing. MPR: Investigation, supervision, writing—review and editing. BL: Investigation, methodology, supervision, writing—review and editing. CMP: Conceptualization, data curation, formal analysis, funding acquisition, investigation, project administration, resources, supervision, visualization, writing—original draft, writing—review and editing, guarantor.

Funding This work was supported by NCI F31 CA232646-01A1 and Hollings Cancer Center Graduate Fellowship (ASS), NIDCR K08 DE26542 and SCTR UL1TR001450 (DMN), Hollings Cancer Center Proteomics Pilot Award (ASS and CP), NCI R01 CA175061, R01 CA208514 (CP).

Competing interests No, there are no competing interests.

Patient consent for publication Not applicable.

Ethics approval Clinical samples were collected after patients gave informed consent and were de-identified prior to transfer to the research laboratory. The Institutional Review Board at the Medical University of South Carolina approved all studies prior to initiation (Approval #00082245). Participants gave informed consent to participate in the study before taking part.

Provenance and peer review Not commissioned; externally peer reviewed.

Data availability statement Data are available in a public, open access repository. All data relevant to the study are included in the article or uploaded as supplementary information. Proteomics data generated from mass spectrometry analysis have been deposited to the ProteomeXchange Consortium via the PRIDE partner repository with the data set identifier PXD022909.

ORCID iDs
Aubrey S Smith http://orcid.org/0000-0003-3693-4262
Eric Bartee http://orcid.org/0000-0003-1793-446X

REFERENCES

1 Rosenberg SA, Restifo NP. Adoptive cell transfer as personalized immunotherapy for human cancer. *Science* 2015;348:62–8.
2 Cheever MA, Greenberg PD, Fefer A. Specificity of adoptive chemoimmunotherapy of established syngeneic tumors. *J Immunol* 1980;125:711–4.
3 Gattinoni L, Finkelstein SE, Klebanoff CA, *et al*. Removal of homeostatic cytokine sinks by lymphodepletion enhances the efficacy of adoptively transferred tumor-specific CD8+ T cells. *J Exp Med* 2005;202:907–12.
4 Antony PA, Piccirillo CA, Akpinarli A, *et al*. CD8+ T cell immunity against a tumor/self-antigen is augmented by CD4+ T helper cells and hindered by naturally occurring T regulatory cells. *J Immunol* 2005;174:2591–601.
5 Ugel S, Peranzoni E, Desantis G, *et al*. Immune tolerance to tumor antigens occurs in a specialized environment of the spleen. *Cell Rep* 2012;2:628–39.
6 Paulos CM, Wrzesinski C, Kaiser A, *et al*. Microbial translocation augments the function of adoptively transferred self/tumor-specific CD8+ T cells via TLR4 signaling. *J Clin Invest* 2007;117:2197–204.
7 Dowling JK, Mansell A. Toll-like receptors: the swiss army knife of immunity and vaccine development. *Clin Transl Immunology* 2016;5:e85.
8 Shekarian T, Valsesia-Wittmann S, Brody J, *et al*. Pattern recognition receptors: immune targets to enhance cancer immunotherapy. *Ann Oncol* 2017;28:1756–66.
9 Nelson MH, Bowers JS, Bailey SR, *et al*. Toll-like receptor agonist therapy can profoundly augment the antitumor activity of adoptively transferred CD8(+) T cells without host preconditioning. *J Immunother Cancer* 2016;4:6.
10 Amos SM, Pegram HJ, Westwood JA, *et al*. Adoptive immunotherapy combined with intratumoral TLR agonist delivery eradicates established melanoma in mice. *Cancer Immunol Immunother* 2011;60:671–83.
11 Dajon M, Iribarren K, Cremer I. Toll-like receptor stimulation in cancer: a pro- and anti-tumor double-edged sword. *Immunobiology* 2017;222:89–100.
12 Speiser DE, Liénard D, Rufer N, *et al*. Rapid and strong human CD8+ T cell responses to vaccination with peptide, IFA, and CpG oligodeoxynucleotide 7909. *J Clin Invest* 2005;115:739–46.
13 Valmori D, Souleimanian NE, Tosello V, *et al*. Vaccination with NY-ESO-1 protein and CpG in Montanide induces integrated antibody/Th1 responses and CD8 T cells through cross-priming. *Proc Natl Acad Sci U S A* 2007;104:8947–52.
14 Karbach J, Gnjatic S, Bender A, *et al*. Tumor-reactive CD8+ T-cell responses after vaccination with NY-ESO-1 peptide, CpG 7909 and Montanide ISA-51: association with survival. *Int J Cancer* 2010;126:909–18.
15 Ribas A, Medina T, Kummar S, *et al*. SD-101 in combination with pembrolizumab in advanced melanoma: results of a phase Ib, multicenter study. *Cancer Discov* 2018;8:1250–7.
16 Weber JS, Zarour H, Redman B, *et al*. Randomized phase 2/3 trial of CpG oligodeoxynucleotide PF-3512676 alone or with dacarbazine for patients with unresectable stage III and IV melanoma. *Cancer* 2009;115:3944–54.
17 Ruzsa A, Sen M, Evans M, *et al*. Phase 2, open-label, 1:1 randomized controlled trial exploring the efficacy of EMD 1201081 in combination with cetuximab in second-line cetuximab-naïve patients with recurrent or metastatic squamous cell carcinoma of the head and neck (r/m SCCHN). *Invest New Drugs* 2014;32:1278–84.
18 Frank MJ, Reagan PM, Bartlett NL, *et al*. *In Situ* vaccination with a TLR9 agonist and local low-dose radiation induces systemic responses in untreated indolent lymphoma. *Cancer Discov* 2018;8:1258–69.
19 Brody JD, Ai WZ, Czerwinski DK, *et al*. In situ vaccination with a TLR9 agonist induces systemic lymphoma regression: a phase I/II study. *J Clin Oncol* 2010;28:4324–32.
20 Kim YH, Gratzinger D, Harrison C, *et al*. In situ vaccination against mycosis fungoides by intratumoral injection of a TLR9 agonist combined with radiation: a phase 1/2 study. *Blood* 2012;119:355–63.

21 Krieg AM. Development of TLR9 agonists for cancer therapy. *J Clin Invest* 2007;117:1184–94.
22 Haymaker C*et al*. Tilsotolimod with ipilimumab drives tumor responses in anti-PD-1 refractory melanoma. *Cancer Discov* 2021.
23 Engel AL, Holt GE, Lu H. The pharmacokinetics of Toll-like receptor agonists and the impact on the immune system. *Expert Rev Clin Pharmacol* 2011;4:275–89.
24 Hanada K-I, Yu Z, Chappell GR, *et al*. An effective mouse model for adoptive cancer immunotherapy targeting neoantigens. *JCI Insight* 2019;4 doi:10.1172/jci.insight.124405
25 Dudley ME, Wunderlich JR, Shelton TE, *et al*. Generation of tumor-infiltrating lymphocyte cultures for use in adoptive transfer therapy for melanoma patients. *J Immunother* 2003;26:332–42.
26 Cox J, Mann M. MaxQuant enables high peptide identification rates, individualized p.p.b.-range mass accuracies and proteome-wide protein quantification. *Nat Biotechnol* 2008;26:1367–72.
27 Cox J, Hein MY, Luber CA, *et al*. Accurate proteome-wide label-free quantification by delayed normalization and maximal peptide ratio extraction, termed MaxLFQ. *Mol Cell Proteomics* 2014;13:2513–26.
28 Tyanova S, Temu T, Cox J. The MaxQuant computational platform for mass spectrometry-based shotgun proteomics. *Nat Protoc* 2016;11:2301–19.
29 Tyanova S, Temu T, Sinitcyn P, *et al*. The Perseus computational platform for comprehensive analysis of (prote)omics data. *Nat Methods* 2016;13:731–40.
30 Perez-Riverol Y, Csordas A, Bai J, *et al*. The PRIDE database and related tools and resources in 2019: improving support for quantification data. *Nucleic Acids Res* 2019;47:D442–50.
31 Tyanova S, Cox J. Perseus: a bioinformatics platform for integrative analysis of proteomics data in cancer research. *Methods Mol Biol* 2018;1711:133–48.
32 Overwijk WW, Theoret MR, Finkelstein SE, *et al*. Tumor regression and autoimmunity after reversal of a functionally tolerant state of self-reactive CD8+ T cells. *J Exp Med* 2003;198:569–80.
33 Su EW, Moore CJ, Suriano S, *et al*. IL-2Ralpha mediates temporal regulation of IL-2 signaling and enhances immunotherapy. *Sci Transl Med* 2015;7:ra170.
34 Paulos CM, Carpenito C, Plesa G, *et al*. The inducible costimulator (ICOS) is critical for the development of human T_H17 cells. *Sci Transl Med* 2010;2:ra78.
35 Nelson MH, Kundimi S, Bowers JS, *et al*. The inducible costimulator augments Tc17 cell responses to self and tumor tissue. *J Immunol* 2015;194:1737–47.
36 Gupta PK, Godec J, Wolski D, *et al*. CD39 expression identifies terminally exhausted CD8+ T cells. *PLoS Pathog* 2015;11:e1005177.
37 Canale FP, Ramello MC, Núñez N, *et al*. CD39 expression defines cell exhaustion in tumor-infiltrating $CD8^+$ T cells. *Cancer Res* 2018;78:115–28.
38 Rubinstein MP, Cloud CA, Garrett TE, *et al*. Ex vivo interleukin-12-priming during CD8(+) T cell activation dramatically improves adoptive T cell transfer antitumor efficacy in a lymphodepleted host. *J Am Coll Surg* 2012;214:700–7.
39 Barr TA, Brown S, Ryan G, *et al*. TLR-mediated stimulation of APC: distinct cytokine responses of B cells and dendritic cells. *Eur J Immunol* 2007;37:3040–53.
40 Gray RC, Kuchtey J, Harding CV. CpG-B ODNs potently induce low levels of IFN-alphabeta and induce IFN-alphabeta-dependent MHC-I cross-presentation in DCs as effectively as CpG-A and CpG-C ODNs. *J Leukoc Biol* 2007;81:1075–85.
41 Ma L, Zhao G, Hua C, *et al*. Down-regulation of TLR9 expression affects the maturation and function of murine bone marrow-derived dendritic cells induced by CpG. *Cell Mol Immunol* 2009;6:199–205.
42 Suek N, Campesato LF, Merghoub T, *et al*. Targeted APC activation in cancer immunotherapy to enhance the Abscopal effect. *Front Immunol* 2019;10:604.
43 Im SJ, Hashimoto M, Gerner MY, *et al*. Defining CD8+ T cells that provide the proliferative burst after PD-1 therapy. *Nature* 2016;537:417–21.
44 Bowers JS, Majchrzak K, Nelson MH, *et al*. PI3Kdelta inhibition enhances the antitumor fitness of adoptively transferred $CD8^+$ T cells. *Front Immunol* 2017;8:1221.
45 Fu T, He Q, Sharma P. The ICOS/ICOSL pathway is required for optimal antitumor responses mediated by anti-CTLA-4 therapy. *Cancer Res* 2011;71:5445–54.
46 Vigano S, Alatzoglou D, Irving M, *et al*. Targeting adenosine in cancer immunotherapy to enhance T-cell function. *Front Immunol* 2019;10:925.
47 Fang F, Yu M, Cavanagh MM, *et al*. Expression of CD39 on activated T cells impairs their survival in older individuals. *Cell Rep* 2016;14:1218–31.
48 Krishna S, Lowery FJ, Copeland AR, *et al*. Stem-like CD8 T cells mediate response of adoptive cell immunotherapy against human cancer. *Science* 2020;370:1328–34.
49 Pearce EL, Walsh MC, Cejas PJ, *et al*. Enhancing CD8 T-cell memory by modulating fatty acid metabolism. *Nature* 2009;460:103–7.
50 van der Windt GJW, Everts B, Chang C-H, *et al*. Mitochondrial respiratory capacity is a critical regulator of CD8+ T cell memory development. *Immunity* 2012;36:68–78.
51 van der Windt GJW, O'Sullivan D, Everts B, *et al*. CD8 memory T cells have a bioenergetic advantage that underlies their rapid recall ability. *Proc Natl Acad Sci U S A* 2013;110:14336–41.
52 Cabrita R, Lauss M, Sanna A, *et al*. Tertiary lymphoid structures improve immunotherapy and survival in melanoma. *Nature* 2020;577:561–5.
53 Helmink BA, Reddy SM, Gao J, *et al*. B cells and tertiary lymphoid structures promote immunotherapy response. *Nature* 2020;577:549–55.
54 Petitprez F, de Reyniès A, Keung EZ, *et al*. B cells are associated with survival and immunotherapy response in sarcoma. *Nature* 2020;577:556–60.
55 Bruno TC, Ebner PJ, Moore BL, *et al*. Antigen-presenting intratumoral B cells affect $CD4^+$ TIL phenotypes in non-small cell lung cancer patients. *Cancer Immunol Res* 2017;5:898–907.